

Supporting Information

Bidirectional photomagnetism, exciplex fluorescence and dielectric anomalies in a spin crossover Hofmann-type coordination polymer

Yan-Ru Chen, Ting-Ting Ying, Yan-Cong Chen, Pei-Yu Liao, Zhao-Ping Ni* and Ming-Liang Tong*

Key Laboratory of Bioinorganic and Synthetic Chemistry of Ministry of Education, School of Chemistry,
IGCME, Guangdong Basic Research Center of Excellence for Functional Molecular Engineering, Sun
Yat-Sen University, Guangzhou 510275, P. R. China.

Table S1. Crystallographic data and structural refinements for **1** at different temperatures.

Compound	1				
Temperature/ K	260	203	198	145	100
Empirical formula	C ₆₄ H ₃₆ Au ₄ Fe ₂ N ₁₆ O ₂	C ₆₄ H ₃₆ Au ₄ Fe ₂ N ₁₆ O ₂	C ₁₂₈ H ₇₂ Au ₈ Fe ₄ N ₃₂ O ₄	C ₁₂₈ H ₇₂ Au ₈ Fe ₄ N ₃₂ O ₄	C ₁₂₈ H ₇₂ Au ₈ Fe ₄ N ₃₂ O ₄
Formula weight	1960.65	1960.65	3921.30	3921.30	3921.30
Crystal system	Orthorhombic	Orthorhombic	Orthorhombic	Orthorhombic	Orthorhombic
Space group	Pbca	Pbca	P2 ₁ 2 ₁ 2 ₁	P2 ₁ 2 ₁ 2 ₁	P2 ₁ 2 ₁ 2 ₁
<i>a</i> / Å	15.3128(6)	27.6016(6)	15.2903(10)	15.0987(8)	15.0208(9)
<i>b</i> / Å	28.0479(10)	28.7074(8)	27.605(2)	27.5674(15)	27.2962(17)
<i>c</i> / Å	28.7796(11)	15.3460(5)	28.6786(16)	28.4870(15)	28.3700(17)
Volume / Å ³	12360.6(8)	12159.7(6)	12105.1(14)	11857.2(11)	11632.0(12)
<i>Z</i>	8	8	4	4	4
reflns collected	129891	34290	40681	158329	189366
Indep reflns	14140	13240	20643	20863	26582
GOF	1.114	1.139	1.065	1.070	1.061
<i>R</i> ₁ ^a (<i>I</i> >=2σ(<i>I</i>))	0.0468,	0.0956,	0.0698,	0.0332,	0.0404,
w <i>R</i> ₂ ^b (<i>I</i> >=2σ(<i>I</i>))	0.0886	0.1804	0.1401	0.0712	0.0796
<i>R</i> _{int}	0.0702	0.1585	0.1095	0.0448	0.0679
Largest diff. peak/hole / eÅ ⁻³	1.218 / -1.288	3.128 / -3.636	1.900 / -2.738	1.942 / -1.152	1.739 / -1.189
CCDC	2322894	2345335	2345336	2322895	2322896

^a*R*₁ = Σ |F_o| - |F_c| | / Σ |F_o|; ^bw*R*₂ = [Σw(F_o² - F_c²)² / Σw(F_c²)²]^{1/2}.

Table S2. Crystallographic data and structural refinements for **2** at different temperatures.

Compound	2				
Temperature / K	260	203	198	145	100
Empirical formula	C ₆₄ H ₃₆ Au ₄ N ₁₆ O ₂ Zn ₂	C ₆₄ H ₃₆ Au ₄ N ₁₆ O ₂ Zn ₂	C ₆₄ H ₃₆ Au ₄ N ₁₆ O ₂ Zn ₂	C ₆₄ H ₃₆ Au ₄ N ₁₆ O ₂ Zn ₂	C ₆₄ H ₃₆ Au ₄ N ₁₆ O ₂ Zn ₂
Formula weight	1979.69	1979.69	1979.69	1979.69	1979.69
Crystal system	Orthorhombic	Orthorhombic	Orthorhombic	Orthorhombic	Orthorhombic
Space group	Pbca	Pbca	Pbca	Pbca	Pbca
a / Å	15.3822(2)	15.4294(11)	15.4018(12)	15.4048(13)	15.4041(12)
b / Å	27.8326(4)	27.7081(2)	27.7406(2)	27.6851(2)	27.6501(2)
c / Å	28.7255(4)	28.7128(2)	28.6941(2)	28.6645(2)	28.6347(2)
Volume / Å ³	12298.2(3)	12275.28(16)	12259.68(16)	12224.95(17)	12196.27(16)
Z	8	8	8	8	8
reflns collected	42694	138001	123313	125252	123545
Indep reflns	12791	12954	10827	10796	10772
GOF	1.013	1.299	1.064	1.116	1.136
R ₁ ^a (I>=2σ(I))	0.0293	0.0700	0.0328	0.0458	0.0547
wR ₂ ^b (I>=2σ(I))	0.0764	0.1371	0.0800	0.1359	0.1547
R _{int}	0.0391	0.0739	0.0373	0.0513,	0.0606
Largest diff. peak/hole / eÅ ⁻³	1.184 / -0.890	1.872 / -1.572	1.468 / -1.859	2.278 / -3.172	2.925 / -3.630
CCDC	2340544	2352146	2352148	2352147	2352145

^aR₁ = Σ |F_o| - |F_c| | / Σ |F_o|; ^bwR₂ = [Σw(F_o² - F_c²)² / Σw(F_o²)²]^{1/2}.

Table S3. Selected structural parameters of **1** at different temperatures.

Parameter	260 K		203 K		198 K		145 K		100 K	
$\langle \text{Fe-N} \rangle^{\text{a}} / \text{\AA}$	$\langle \text{Fe1-N} \rangle$	2.165	$\langle \text{Fe1-N} \rangle$	2.100	$\langle \text{Fe1-N} \rangle$	2.015	$\langle \text{Fe1-N} \rangle$	1.960	$\langle \text{Fe1-N} \rangle$	1.960
	$\langle \text{Fe2-N} \rangle$	2.170	$\langle \text{Fe2-N} \rangle$	2.166	$\langle \text{Fe2-N} \rangle$	2.155	$\langle \text{Fe2-N} \rangle$	2.013	$\langle \text{Fe2-N} \rangle$	1.988
	$\langle \text{Fe3-N} \rangle$		$\langle \text{Fe3-N} \rangle$		$\langle \text{Fe3-N} \rangle$	2.160	$\langle \text{Fe3-N} \rangle$	2.160	$\langle \text{Fe3-N} \rangle$	2.160
$\sum \text{Fe}^{\text{b}} / {}^\circ$	ΣFe1	18.17	ΣFe1	21.36	ΣFe1	20.34	ΣFe1	17.29	ΣFe1	16.67
	ΣFe2	14.04	ΣFe2	17.67	ΣFe2	21.99	ΣFe2	9.08	ΣFe2	11.07
	ΣFe3		ΣFe3		ΣFe3	21.10	ΣFe3	21.19	ΣFe3	22.00
$\text{Fe-N}\equiv\text{C}^{\text{c}} / {}^\circ$	$\text{Fe1-N}\equiv\text{C}$	171.58	$\text{Fe1-N}\equiv\text{C}$	172.1	$\text{Fe1-N}\equiv\text{C}$	173.3	$\text{Fe1-N}\equiv\text{C}$	174.6	$\text{Fe1-N}\equiv\text{C}$	174.5
	$\text{Fe2-N}\equiv\text{C}$	166.94	$\text{Fe2-N}\equiv\text{C}$	167.5	$\text{Fe2-N}\equiv\text{C}$	167.5	$\text{Fe2-N}\equiv\text{C}$	171.6	$\text{Fe2-N}\equiv\text{C}$	171.9
	$\text{Fe3-N}\equiv\text{C}$		$\text{Fe3-N}\equiv\text{C}$		$\text{Fe3-N}\equiv\text{C}$	164.5	$\text{Fe3-N}\equiv\text{C}$	165.4	$\text{Fe3-N}\equiv\text{C}$	164.8
$\text{Fe}\cdots\text{Fe}^{\text{d}} / \text{\AA}$	Fe1-Fe2	10.43	Fe1-Fe2	10.38	Fe1-Fe2	10.23	Fe1-Fe2	10.09	Fe1-Fe2	10.08
		10.38		10.33	Fe1-Fe2	10.20	Fe1-Fe2	10.06	Fe1-Fe2	10.05
		10.36		10.30	Fe1-Fe3	10.30	Fe1-Fe3	10.24	Fe1-Fe3	10.23
		10.35		10.28	Fe1-Fe3	10.22	Fe1-Fe3	10.17	Fe1-Fe3	10.17

^aThe average Fe-N bond lengths; ^bOctahedral distortion parameters; ^cAverage Fe-N≡C angles within Hofmann layer; ^dThe Fe···Fe distances linked by [Au(CN)₂]⁻.

	Fe1-Fe1	14.39	Fe1-Fe1	14.36	Fe1-Fe4	14.33	Fe1-Fe4	14.25	Fe1-Fe4	14.20
Fe...Fe ^e / Å	Fe2-Fe2	14.39	Fe2-Fe2	14.36	Fe3-Fe3	14.35	Fe3-Fe3	14.25	Fe3-Fe3	14.19
	L1	2.88	L1	4.30	L1	1.22	L1	14.53	L1	19.02
		5.61		3.71		3.75		4.82		4.45
Dihedral angle ^f / °	L2	12.89	L2	4.30	L2	12.57	L2	21.17	L2	12.70
		13.46		3.71		11.78		21.17		10.35
					L3	27.21	L3	31.13	L3	32.47
						16.05		31.13		15.54
					L4	7.15	L4	14.53	L4	5.01
						2.33		4.82		2.34
Au...Au ^g / Å	Au1-Au3	3.09	Au1-Au2	3.10	Au1-Au6	3.08	Au1-Au6	3.05	Au1-Au6	3.05
	Au2-Au4	3.03	Au3-Au4	3.02	Au2-Au3	3.01	Au2-Au3	3.01	Au2-Au3	2.99
					Au4-Au5	3.02	Au4-Au5	2.99	Au4-Au5	2.97
					Au7-Au8	3.10	Au7-Au8	3.11	Au7-Au8	3.08

^eDistances between Fe...Fe connected by dpoda ligand; ^fThe dihedral angles between the 1,3,4-oxadiazole and each pyridine ring in dpoda ligands, in which the labels of ligands (L) are same as the labels on the oxygen atoms; ^gThe shortest Au...Au distance between the neighboring Hofmann layers.

Table S4. Selected structural parameters of **2** at different temperatures.

Parameter	260 K		203 K		198 K		145 K		100 K	
$\langle \text{Zn-N} \rangle^{\text{a}} / \text{\AA}$	$\langle \text{Zn1-N} \rangle$	2.154	$\langle \text{Zn1-N} \rangle$	2.150	$\langle \text{Zn1-N} \rangle$	2.150	$\langle \text{Zn1-N} \rangle$	2.150	$\langle \text{Zn1-N} \rangle$	2.148
	$\langle \text{Zn2-N} \rangle$	2.157	$\langle \text{Zn2-N} \rangle$	2.155	$\langle \text{Zn2-N} \rangle$	2.155	$\langle \text{Zn2-N} \rangle$	2.152	$\langle \text{Zn2-N} \rangle$	2.149
$\Sigma \text{Zn}^{\text{b}} / {}^\circ$	ΣZn1	18.70	ΣZn1	20.57	ΣZn1	19.50	ΣZn1	20.34	ΣZn1	21.76
	ΣZn2	17.08	ΣZn2	18.67	ΣZn2	18.21	ΣZn2	16.81	ΣZn2	17.68
$\text{Zn-N}\equiv\text{C}^{\text{c}} / {}^\circ$	$\text{Zn1-N}\equiv\text{C}$	171.05	$\text{Zn1-N}\equiv\text{C}$	170.88	$\text{Zn1-N}\equiv\text{C}$	171.05	$\text{Zn1-N}\equiv\text{C}$	170.75	$\text{Zn1-N}\equiv\text{C}$	170.83
	$\text{Zn2-N}\equiv\text{C}$	166.35	$\text{Zn2-N}\equiv\text{C}$	165.90	$\text{Zn2-N}\equiv\text{C}$	166.23	$\text{Zn2-N}\equiv\text{C}$	166.23	$\text{Zn2-N}\equiv\text{C}$	166.13
$\text{Zn}\cdots\text{Zn}^{\text{d}} / \text{\AA}$	Zn1-Zn2	10.37	Zn1-Zn2	10.37	Zn1-Zn2	10.37	Zn1-Zn2	10.36	Zn1-Zn2	10.35
$\text{Zn}\cdots\text{Zn}^{\text{e}} / \text{\AA}$	Zn1-Zn1	14.37	Zn1-Zn1	14.35	Zn1-Zn1	14.36	Zn1-Zn1	14.34	Zn1-Zn1	14.32
	L1	6.41	L1	6.35	L1	6.25	L1	6.27	L1	5.71
		2.50		2.62		2.60		2.33		2.42
	L2	13.81	L2	12.71	L2	13.30	L2	13.02	L2	12.89
		13.21		13.40		12.63		13.31		13.10
$\text{Au}\cdots\text{Au}^{\text{g}} / \text{\AA}$	Au1-Au4	3.10	Au1-Au4	3.09	Au1-Au4	3.09	Au1-Au4	3.09	Au1-Au4	3.08
	Au2-Au3	3.03	Au2-Au3	3.03	Au2-Au3	3.03	Au2-Au3	3.03	Au2-Au3	3.02

^aThe average Zn-N bond lengths; ^bOctahedral distortion parameters; ^cAverage Zn-N≡C angles within Hofmann layer; ^dThe Zn...Zn distances linked by $[\text{Au}(\text{CN})_2]^-$. ^eDistances between Zn...Zn connected by dpoda ligand; ^fThe dihedral angles between the 1,3,4-oxadiazole and each pyridine ring in dpoda ligands, in which the labels of ligands (L) are same as the labels on the oxygen atoms; ^gThe shortest Au...Au distance between the neighboring Hofmann layers.

Table S5. Offset face-to-face $\pi\cdots\pi$ interactions in **1** at 260 K.

260 K	$\Theta^{[1]} (\text{°})$	$Z^{[2]} (\text{\AA})$	260 K	$\Theta (\text{°})$	$Z (\text{\AA})$
Part 1 ^[3]			Part 2		
L3-b ^[4] (C6 C7 N2 N3 O1) G3-b (C41A C42A C43A C44A C45A C46A)	8.06	3.72	L3-b (C6 C7 N2 N3 O1) G3-b (C36 C37 C42 C43 C47 C48)	2.74	3.83
L3-c (C1 C2 C3 C4 C5 N1) G3-c (C35A C42A C43A C44A C45A C46A)	7.68	3.92	L3-c (C1 C2 C3 C4 C5 N1) G3-c (C41 C42 C43 C44 C45 C46)	3.13	3.93
L3-b' (C6 C7 N2 N3 O1) G3-d (C34A C35A C39A C40A C41A C42A)	6.07	3.61	L3-b' (C6 C7 N2 N3 O1) G3-d (C35 C36 C39 C40 C41 C42)	4.45	3.67
L3-c' (C1 C2 C3 C4 C5 N1) G3-a (C33A C34A C35A C37A C38A C43A)	5.81	3.92	L3-c' (C1 C2 C3 C4 C5 N1) G3-a (C33 C34 C35 C36 C37 C38)	1.79	3.77
L3-b'' (C6 C7 N2 N3 O1) G3-c' (C35A C42A C43A C44A C45A C46A)	7.39	3.87			

^[1] The dihedral angle between two aromatic rings; ^[2] The distance between the centroids of aromatic rings. ^[3] The pyrene guest G3 is disordered over two positions with a ratio of 39:61, which are shown in part 1 and part 2, respectively. ^[4] L and G denote the dpoda ligand and pyrene guest, respectively. Numbers and letters are used to mark different aromatic rings shown in Figure S12. Symmetry Codes: L3-b', L3-c': 1-x, 1-y, 1-z; L3-b'', G3-c': 1/2-x, 1-y, -1/2+z.

Table S6. C-H···π interactions in **1** at 260 K.

260 K	$\Theta^{[1]} (\text{°})$	$Z^{[2]} (\text{\AA})$	260 K	$\Theta (\text{°})$	$Z (\text{\AA})$
Part 1 ^[3]			Part 2		
G1-b ^[4] (C52 C53 C58 C59 C63 C64) G3-a (C33A C34A C35A C37A C38A C43A)	84.51	5.09	G1-b (C52 C53 C58 C59 C63 C64) G3-a (C33 C34 C35 C36 C37 C38)	89.37	5.01
G1-b' (C52 C53 C58 C59 C63 C64) G3-a' (C33A C34A C35A C37A C38A C43A)	84.51	5.09	G1-c' (C57 C58 C59 C60 C61 C62) G3-a' (C33 C34 C35 C36 C37 C38)	89.46	5.46
L1-b'' (C24 C25 N11 N12 O2) L3-c' (C1 C2 C3 C4 C5 N1)	66.73	5.48	L1-b'' (C24 C25 N11 N12 O2) L3-c' (C1 C2 C3 C4 C5 N1)	66.73	5.48
G1-d (C51 C52 C55 C56 C57 C58) L3-c' (C1 C2 C3 C4 C5 N1)	89.09	5.35	G1-d (C51 C52 C55 C56 C57 C58) L3-c' (C1 C2 C3 C4 C5 N1)	89.69	5.01

^[1] The dihedral angle between two aromatic rings; ^[2] The distance between the centroids of aromatic rings. ^[3] The pyrene guest G3 is disordered over two positions with a ratio of 39:61, which are shown in part 1 and part 2, respectively. ^[4] L and G denote the dpoda ligand and pyrene guest, respectively. Numbers and letters are used to mark different aromatic rings shown in Figure S12. Symmetry Codes: G1-b': -1/2+x, 1/2-y, 1-y; G3-a': 1/2-x, 1-y, -1/2+z; L1-b'': 1/2-x, 1-y, -1/2+z; L3-c': 1-x, 1-y, 1-z.

Table S7. Offset face-to-face $\pi\cdots\pi$ interactions in **2** at 260 K.

260 K	$\Theta^{[1]} (\text{°})$	$Z^{[2]} (\text{\AA})$	260 K	$\Theta (\text{°})$	$Z (\text{\AA})$
Part 1 ^[3]			Part 2		
L1-b ^[4] (C20 C21 N7 N8 O2) G1-a (C35 C36 C39 C40 C41 C42)	19.06	4.00	L1-b (C20 C21 N7 N8 O2) G1-a (C35 C36 C39 C40 C41 C42)	19.06	4.00
L3-b (C6 C7 N2 N3 O1) G3-c (C52 C53 C58 C59 C63 C54)	6.95	3.76	L3-b (C6 C7 N2 N3 O1) G3-c (C51A C52A C55A C56A C57A C58A)	4.50	3.81
L3-c (C1 C2 C3 C4 C5 N1) G3-b (C49 C50 C51 C52 C53 C54)	7.55	3.92	L3-c (C1 C2 C3 C4 C5 N1) G3-b (C49A C50A C51A C52A C53A C54A)	4.07	3.89
L3-b' (C6 C7 N2 N3 O1) G3-a (C51 C52 C55 C56 C57 C58)	7.57	3.60	L3-b' (C6 C7 N2 N3 O1) G3-a (C52A C53A C58A C59A C63A C64A)	4.72	3.64
L3-c' (C1 C2 C3 C4 C5 N1) G3-d (C57 C58 C59 C60 C61 C62)	4.27	3.95	L3-c' (C1 C2 C3 C4 C5 N1) G3-d (C57A C58A C59A C60A C61A C62A)	3.23	3.75

^[1] The dihedral angle between two aromatic rings; ^[2] The distance between the centroids of aromatic rings. ^[3] The pyrene guest G3 is disordered over two positions with a ratio of 50:50, which are shown in part 1 and part 2, respectively. ^[4] L and G denote the dpoda ligand and pyrene guest, respectively. Numbers and letters are used to mark different aromatic rings shown in Figure S13. Symmetry Codes: L3-b', L3-c': -1/2+x, x, 1/2-y.

Table S8. C-H···π interactions in **2** at 260 K.

260 K	$\Theta^{[1]} (\text{°})$	$Z^{[2]} (\text{\AA})$	260 K	$\Theta (\text{°})$	$Z (\text{\AA})$
Part 1 ^[3]			Part 2		
G1-c ^[4] (C36 C37 C42 C43 C47 C48) G3-d (C57 C58 C59 C60 C61 C62)	86.07	5.05	G1-c (C36 C37 C42 C43 C47 C48) G3-d (C57A C58A C59A C60A C61A C62A)	87.17	4.96
L1-b'' (C20 C21 N7 N8 O2) L3-c' (C1 C2 C3 C4 C5 N1)	66.45	5.46	L1-b'' (C20 C21 N7 N8 O2) L3-c' (C1 C2 C3 C4 C5 N1)	66.45	5.46
G1-a (C35 C36 C39 C40 C41 C42) L3-c' (C1 C2 C3 C4 C5 N1)	89.72	5.31	G1-a (C35 C36 C39 C40 C41 C42) L3-c' (C1 C2 C3 C4 C5 N1)	89.72	5.31

^[1] The dihedral angle between two aromatic rings; ^[2] The distance between the centroids of aromatic rings. ^[3] The pyrene guest G3 is disordered over two positions with a ratio of 50:50, which are shown in part 1 and part 2, respectively. ^[4] L and G denote the dpoda ligand and pyrene guest, respectively. Numbers and letters are used to mark different aromatic rings shown in Figure S13. Symmetry Codes: L1-b'':1/2-x, 1/2+y, z; L3-c':-1/2+x, y, 1/2-z.

Table S9. Offset face-to-face $\pi\cdots\pi$ interactions in **1** at 203 K.

203 K	$\Theta^{[1]} (\circ)$	$Z^{[2]} (\text{\AA})$	203 K	$\Theta (\circ)$	$Z (\text{\AA})$
Part 1 ^[3]			Part 2		
L3-b ^[4] (C6 C7 N2 N3 O1) G3-c (C53 C54 C55 C56 C57 C58)	9.81	3.73	L3-b (C6 C7 N2 N3 O1) G3-c (C49A C50A C51A C52A C53A C54A)	4.15	3.81
L3-c (C8 C9 C10 C11 C12 N4) G3-b (C52 C53 C58 C59 C60 C61)	8.69	3.90	L3-c (C8 C9 C10 C11 C12 N4) G3-b (C51A C52A C61A C62A C63A C64A)	3.43	3.93
L3-b' (C6 C7 N2 N3 O1) G3-a (C51 C52 C61 C62 C63 C64)	8.01	3.56	L3-b' (C6 C7 N2 N3 O1) G3-a (C52A C53A C58A C59A C60A C61A)	4.41	3.62
L3-c' (C8 C9 C10 C11 C12 N4) G3-d (C49 C50 C51 C52 C53 C54)	5.53	3.97	L3-c' (C8 C9 C10 C11 C12 N4) G3-d (C53A C54A C55A C56A C57A C58A)	4.37	3.75

^[1] The dihedral angle between two aromatic rings; ^[2] The distance between the centroids of aromatic rings. ^[3] The pyrene guest G3 is disordered over two positions with a ratio of 59:41, which are shown in part 1 and part 2, respectively. ^[4] L and G denote the dpoda ligand and pyrene guest, respectively. Numbers and letters are used to mark different aromatic rings shown in Figure S14. Symmetry Codes: L3-b': 3/2-x, -1/2+y, z.

Table S10. C-H···π interactions in **1** at 203 K.

203 K	$\Theta^{[1]} (\text{°})$	$Z^{[2]} (\text{\AA})$	203 K	$\Theta (\text{°})$	$Z (\text{\AA})$
Part 1 ^[3]			Part 2		
G1-c ^[4] (C37 C38 C39 C40 C41 C42) G3-d (C49 C50 C51 C52 C53 C54)	85.05	5.01	G1-c (C37 C38 C39 C40 C41 C42) G3-d (C53A C54A C55A C56A C57A C58A)	86.23	4.88
L3-c' ^[4] (C8 C9 C10 C11 C12 N4) L1-b'' (C26 C27 N14 N15 O2)	67.48	5.43	L3-c' (C8 C9 C10 C11 C12 N4) L1-b'' (C26 C27 N14 N15 O2)	67.48	5.43
G1-a (C36 C37 C42 C43 C47 C48) L3-c' (C8 C9 C10 C11 C12 N4)	89.37	5.26	G1-a (C36 C37 C42 C43 C47 C48) L3-c' (C8 C9 C10 C11 C12 N4)	89.37	5.26

^[1] The dihedral angle between two aromatic rings; ^[2] The distance between the centroids of aromatic rings. ^[3] The pyrene guest G3 is disordered over two positions with a ratio of 59:41, which are shown in part 1 and part 2, respectively. ^[4] L and G denote the dpoda ligand and pyrene guest, respectively. Numbers and letters are used to mark different aromatic rings shown in Figure S14. Symmetry Codes: L3-c': 3/2-x, -1/2+y, z; L1-b'': 1/2+x, 1/2-y, -z.

Table S11. Offset face-to-face $\pi\cdots\pi$ interactions in **2** at 203 K.

203 K	$\Theta^{[1]} (\circ)$	$Z^{[2]} (\text{\AA})$	203 K	$\Theta (\circ)$	$Z (\text{\AA})$
Part 1 ^[3]			Part 2		
L1-b ^[4] (C20 C21 N7 N8 O2) G1-a (C35 C36 C39 C40 C41 C42)	18.08	3.98	L1-b (C20 C21 N7 N8 O2) G1-a (C35 C36 C39 C40 C41 C42)	18.08	3.98
L3-b (C6 C7 N2 N3 O1) G3-c (C57 C58 C59 C60 C61 C62)	6.88	3.77	L3-b (C6 C7 N2 N3 O1) G3-c (C51A C52A C55A C56A C57A C58A)	5.11	3.79
L3-c (C1 C2 C3 C4 C5 N1) G3-b (C52 C53 C58 C59 C63 C64)	7.09	3.92	L3-c (C1 C2 C3 C4 C5 N1) G3-b (C49A C50A C51A C52A C53A C54A)	4.65	3.91
L3-b' (C6 C7 N2 N3 O1) G3-a (C49 C50 C51 C52 C53 C54)	7.31	3.58	L3-b' (C6 C7 N2 N3 O1) G3-a (C52A C53A C58A C59A C63A C64A)	4.38	3.64
L3-c' (C1 C2 C3 C4 C5 N1) G3-d (C51 C52 C55 C56 C57 C58)	5.97	3.94	L3-c' (C1 C2 C3 C4 C5 N1) G3-d (C57A C58A C59A C60A C61A C62A)	2.39	3.75

^[1] The dihedral angle between two aromatic rings; ^[2] The distance between the centroids of aromatic rings. ^[3] The pyrene guest G3 is disordered over two positions with a ratio of 50:50, which are shown in part 1 and part 2, respectively. ^[4] L and G denote the dpoda ligand and pyrene guest, respectively. Numbers and letters are used to mark different aromatic rings shown in Figure S15. Symmetry Codes: L3-b', L3-c': -1/2+x, 1+y, 1/2-z.

Table S12. C-H···π interactions in **2** at 203 K.

203 K	$\Theta^{[1]} (\text{°})$	$Z^{[2]} (\text{\AA})$	203 K	$\Theta (\text{°})$	$Z (\text{\AA})$
Part 1 ^[3]			Part 2		
G1-c ^[4] (C36 C37 C42 C43 C47 C48) G3-d (C51 C52 C55 C56 C57 C58)	82.95	5.01	G1-c (C36 C37 C42 C43 C47 C48) G3-d (C57A C58A C59A C60A C61A C62A)	86.66	4.96
L3-c' ^[4] (C1 C2 C3 C4 C5 N1) L1-b'' (C20 C21 N6 N7 O2)	65.24	5.44	L3-c' (C1 C2 C3 C4 C5 N1) L1-b'' (C20 C21 N6 N7 O2)	65.24	5.44
G1-a (C35 C36 C39 C40 C41 C42) L3-c' (C1 C2 C3 C4 C5 N1)	87.74	5.30	G1-a (C35 C36 C39 C40 C41 C42) L3-c' (C1 C2 C3 C4 C5 N1)	87.74	5.30

^[1] The dihedral angle between two aromatic rings; ^[2] The distance between the centroids of aromatic rings. ^[3] The pyrene guest G3 is disordered over two positions with a ratio of 50:50, which are shown in part 1 and part 2, respectively. ^[4] L and G denote the dpoda ligand and pyrene guest, respectively. Numbers and letters are used to mark different aromatic rings shown in Figure S15. Symmetry Codes: L3-c': -1/2+x, 1+y, 1/2-z; L1-b'': 1/2-x, 1/2+y, 1+z.

Table S13. Offset face-to-face $\pi\cdots\pi$ interactions in **1** at 198 K.

198 K	$\Theta^{[1]} (\text{°})$	$Z^{[2]} (\text{\AA})$	198 K	$\Theta (\text{°})$	$Z (\text{\AA})$
L1-b ^[3] (C34 C35 N14 N15 O3) G1-a (C117 C118 C119 C120 C121 C122)	16.81	3.94	L4-a (C13 C14 C15 C16 C17 N5) G4-c (C83 C84 C93 C94 C95 C96)	5.10	3.85
L3-b ^[3] (C6 C7 N2 N3 O1) G3-c (C69 C70 C71 C72 C73 C74)	8.35	3.75	L4-b (C18 C19 N6 N7 O2) G4-b (C81 C82 C83 C84 C85 C86)	6.34	3.73
L3-c (C8 C9 C10 C11 C12 N4) G3-b (C68 C69 C74 C75 C76 C77)	7.10	3.89	L3-b' (C6 C7 N2 N3 O1) G4-d (C84 C85 C90 C91 C92 C93)	6.85	3.59
L4-b (C18 C19 N6 N7 O2) G3-a (C67 C68 C77 C78 C79 C80)	8.15	3.62	L3-c' (C8 C9 C10 C11 C12 N4) G4-a (C85 C86 C87 C88 C89 C90)	3.25	3.67

^[1] The dihedral angle between two aromatic rings; ^[2] The distance between the centroids of aromatic rings. ^[3] L and G denote the dpoda ligand and pyrene guest, respectively. Numbers and letters are used to mark different aromatic rings shown in Figure S16. Symmetry Codes: L3-b': -1+x, y, z.

Table S14. C-H···π interactions in **1** at 198 K.

198 K	Θ^[1] (°)	Z^[2] (Å)	198 K	Θ (°)	Z (Å)
G1-c ^[3] (C116 C117 C122 C123 C127 C128)			G1-a (C117 C118 C119 C120 C121 C122)		
G3-d (C65 C66 C67 C68 C69 C70)	83.51	5.00	L4-a (C13 C14 C15 C16 C17 N5)	85.81	5.30
G2-b (C97 C98 C99 C100 C101 C102)	86.85	4.91	L3-c' ^[3] (C8 C9 C10 C11 C12 N4) L1-b' (N14 N15 C34 C35 O3)	64.44	5.42
G2-d (C100 C101 C106 C107 C108 C109)	89.51	5.26	L4-a (C13 C14 C15 C16 C17 N5) L2-b' (C22 C23 C50 C51 O4)	71.87	5.41
L3-c' (C8 C9 C10 C11 C12 N4)					

^[1] The dihedral angle between two aromatic rings; ^[2] The distance between the centroids of aromatic rings. ^[3] L and G denote the dpoda ligand and pyrene guest, respectively. Numbers and letters are used to mark different aromatic rings shown in Figure S16. Symmetry Codes: L3-c': -1+x, y, z; L1-b': -1+x, 1/2+y, 1/2-z.

Table S15. Offset face-to-face $\pi\cdots\pi$ interactions in **2** at 198 K.

198 K	$\Theta^{[1]} (\text{°})$	$Z^{[2]} (\text{\AA})$	198 K	$\Theta (\text{°})$	$Z (\text{\AA})$
Part 1 ^[3]			Part 2		
L1-b ^[4] (C20 C21 N7 N8 O2) G1-a (C35 C36 C39 C40 C41 C42)	18.80	3.99	L1-b (C20 C21 N7 N8 O2) G1-a (C35 C36 C39 C40 C41 C42)	18.80	3.99
L3-b (C6 C7 N2 N3 O1) G3-c (C57 C58 C59 C60 C61 C62)	7.29	3.76	L3-b (C6 C7 N2 N3 O1) G3-c (C51A C52A C55A C56A C57A C58A)	5.24	3.80
L3-c (C1 C2 C3 C4 C5 N1) G3-b (C52 C53 C58 C59 C63 C64)	7.65	3.91	L3-c (C1 C2 C3 C4 C5 N1) G3-b (C49A C50A C51A C52A C53A C54A)	4.01	3.92
L3-b' (C6 C7 N2 N3 O1) G3-a (C49 C50 C51 C52 C53 C54)	7.52	3.58	L3-b' (C6 C7 N2 N3 O1) G3-a (C52A C53A C58A C59A C63A C64A)	4.34	3.64
L3-c' (C1 C2 C3 C4 C5 N1) G3-d (C51 C52 C55 C56 C57 C58)	6.34	3.93	L3-c' (C1 C2 C3 C4 C5 N1) G3-d (C57A C58A C59A C60A C61A C62A)	2.59	3.76

^[1] The dihedral angle between two aromatic rings; ^[2] The distance between the centroids of aromatic rings. ^[3] The pyrene guest G3 is disordered over two positions with a ratio of 50:50, which are shown in part 1 and part 2, respectively. ^[4] L and G denote the dpoda ligand and pyrene guest, respectively. Numbers and letters are used to mark different aromatic rings shown in Figure S17. Symmetry Codes: L3-b': -1/2+x, 1+y, 1/2-z.

Table S16. C-H···π interactions in **2** at 198 K.

198 K	$\Theta^{[1]} (\text{°})$	$Z^{[2]} (\text{\AA})$	203 K	$\Theta (\text{°})$	$Z (\text{\AA})$
Part 1 ^[3]			Part 2		
G1-c ^[4] (C36 C37 C42 C43 C47 C48)	83.37	5.02	G1-c (C36 C37 C42 C43 C47 C48)		
G3-d (C51 C52 C55 C56 C57 C58)			G3-d (C57A C58A C59A C60A C61A C62A)	87.33	4.96
L3-c' ^[4] (C1 C2 C3 C4 C5 N1)	66.26	5.45	L3-c' (C1 C2 C3 C4 C5 N1)		
L1-b'' (C20 C21 N7 N8 O2)			L1-b'' (C20 C21 N7 N8 O2)	66.26	5.45
G1-a (C35 C36 C39 C40 C41 C42)	89.82	5.31	G1-a (C35 C36 C39 C40 C41 C42)		
L3-c' (C1 C2 C3 C4 C5 N1)			L3-c' (C1 C2 C3 C4 C5 N1)	89.82	5.31

^[1] The dihedral angle between two aromatic rings; ^[2] The distance between the centroids of aromatic rings. ^[3] The pyrene guest G3 is disordered over two positions with a ratio of 50:50, which are shown in part 1 and part 2, respectively. ^[4] L and G denote the dpoda ligand and pyrene guest, respectively. Numbers and letters are used to mark different aromatic rings shown in Figure S17. Symmetry Codes: L3-c': -1/2+x, 1+y, 1/2-z; L1-b'': 1/2-x, 1/2+y, z.

Table S17. Offset face-to-face $\pi\cdots\pi$ interactions in **1** at 145 K.

145 K	$\Theta^{[1]}$ (°)	$Z^{[2]}$ (Å)	145 K	Θ (°)	Z (Å)
L1-b ^[3] (C34 C35 N14 N15 O3) G1-a (C117 C118 C119 C120 C121 C122)	15.30	3.85	L4-a (C13 C14 C15 C16 C17 N5) G4-c (C81 C82 C83 C84 C85 C86)	6.67	3.86
L3-b (C6 C7 N2 N3 O1) G3-c (C69 C70 C71 C72 C73 C74)	10.54	3.73	L4-b (C18 C19 N6 N7 O2) G4-b (C83 C84 C93 C94 C95 C96)	2.19	3.68
L3-c (C8 C9 C10 C11 C12 N4) G3-b (C68 C69 C74 C75 C76 C77)	7.62	3.91	L3-b' (C6 C7 N2 N3 O1) G4-d (C85 C86 C87 C88 C89 C90)	7.26	3.54
L4-a (C13 C14 C15 C16 C17 N5) G3-d (C65 C66 C67 C68 C69 C70)	12.19	4.03	L3-c' (C8 C9 C10 C11 C12 N4) G4-a (C84 C85 C90 C91 C92 C93)	1.45	3.65
L4-b (C18 C19 N6 N7 O2) G3-a (C67 C68 C77 C78 C79 C80)	7.20	3.64			

^[1] The dihedral angle between two aromatic rings; ^[2] The distance between the centroids of aromatic rings. ^[3] L and G denote the dpoda ligand and pyrene guest, respectively. Numbers and letters are used to mark different aromatic rings shown in Figure S18. Symmetry Codes: L3-b': -1+x, y, z.

Table S18. C-H···π interactions in **1** at 145 K.

145 K	$\Theta^{[1]} (\text{°})$	$Z^{[2]} (\text{\AA})$	145 K	$\Theta (\text{°})$	$Z (\text{\AA})$
G1-c ^[3] (C116 C117 C122 C123 C127 C128)	82.65	4.90	G1-a (C117 C118 C119 C120 C121 C122)	84.29	5.31
G3-d (C65 C66 C67 C68 C69 C70)			L4-a (C13 C14 C15 C16 C17 N5)		
G2-b (C97 C98 C99 C100 C101 C102) G4-a (C84 C85 C90 C91 C92 C93)	89.31	4.89	L2-b' (C50 C51 N22 N23 O4) L4-a (C13 C14 C15 C16 C17 N5)	75.77	5.41
G2-d (C100 C101 C106 C107 C108 C109) L3-c' (C8 C9 C10 C11 C12 N4)	88.80	5.23	L1-b' (C34 C35 N14 N15 O3) L3-c' (C8 C9 C10 C11 C12 N4)	64.93	5.37

^[1] The dihedral angle between two aromatic rings; ^[2] The distance between the centroids of aromatic rings. ^[3] L and G denote the dpoda ligand and pyrene guest, respectively. Numbers and letters are used to mark different aromatic rings shown in Figure S18.
Symmetry Codes: L3-c': -1+x, y, z; L1-b': -1+x, 1/2+y, 1/2-z.

Table S19. Offset face-to-face $\pi\cdots\pi$ interactions in **2** at 145 K.

145 K	$\Theta^{[1]} (\text{°})$	$Z^{[2]} (\text{\AA})$	145 K	$\Theta (\text{°})$	$Z (\text{\AA})$
Part 1 ^[3]			Part 2		
L1-b ^[4] (C20 C21 N7 N8 O2) G1-a (C35 C36 C39 C40 C41 C42)	18.43	3.99	L1-b (C20 C21 N7 N8 O2) G1-a (C35 C36 C39 C40 C41 C42)	18.43	3.99
L3-b (C6 C7 N2 N3 O1) G3-c (C57 C58 C59 C60 C61 C62)	7.74	3.77	L3-b (C6 C7 N2 N3 O1) G3-c (C51A C52A C55A C56A C57A C58A)	4.92	3.79
L3-c (C1 C2 C3 C4 C5 N1) G3-b (C52 C53 C58 C59 C63 C64)	8.19	3.91	L3-c (C1 C2 C3 C4 C5 N1) G3-b (C49A C50A C51A C52A C53A C54A)	3.66	3.92
L3-b' (C6 C7 N2 N3 O1) G3-a (C49 C50 C51 C52 C53 C54)	8.14	3.57	L3-b' (C6 C7 N2 N3 O1) G3-a (C52A C53A C58A C59A C63A C64A)	4.03	3.67
L3-c' (C1 C2 C3 C4 C5 N1) G3-d (C51 C52 C55 C56 C57 C58)	6.86	3.91	L3-c' (C1 C2 C3 C4 C5 N1) G3-d (C57A C58A C59A C60A C61A C62A)	2.72	3.76

^[1] The dihedral angle between two aromatic rings; ^[2] The distance between the centroids of aromatic rings. ^[3] The pyrene guest G3 is disordered over two positions with a ratio of 50:50, which are shown in part 1 and part 2, respectively. ^[4] L and G denote the dpoda ligand and pyrene guest, respectively. Numbers and letters are used to mark different aromatic rings shown in Figure S19. Symmetry Codes: L3-b', L3-c': -1/2+x, 1+y, 1/2-z.

Table S20. C-H···π interactions in **2** at 145 K.

145 K	$\Theta^{[1]} (\text{°})$	$Z^{[2]} (\text{\AA})$	145 K	$\Theta (\text{°})$	$Z (\text{\AA})$
Part 1 ^[3]			Part 2		
G1-c ^[4] (C36 C37 C42 C43 C47 C48) G3-d (C51 C52 C55 C56 C57 C58)	82.40	4.99	G1-c (C36 C37 C42 C43 C47 C48) G3-d (C57A C58A C59A C60A C61A C62A)	87.11	4.97
L3-c' (C1 C2 C3 C4 C5 N1) L1-b'' (C20 C21 N7 N8 O2)	65.85	5.44	L3-c' (C1 C2 C3 C4 C5 N1) L1-b'' (C20 C21 N7 N8 O2)	65.87	5.44
G1-a (C35 C36 C39 C40 C41 C42) L3-c' (C1 C2 C3 C4 C5 N1)	89.32	5.32	G1-a (C35 C36 C39 C40 C41 C42) L3-c' (C1 C2 C3 C4 C5 N1)	89.32	5.32

^[1] The dihedral angle between two aromatic rings; ^[2] The distance between the centroids of aromatic rings. ^[3] The pyrene guest G3 is disordered over two positions with a ratio of 50:50, which are shown in part 1 and part 2, respectively. ^[4] L and G denote the dpoda ligand and pyrene guest, respectively. Numbers and letters are used to mark different aromatic rings shown in Figure S19. Symmetry Codes: L3-c': -1/2+x, 1+y, 1/2-z; L1-b'': 1/2-x, 1/2+y, z.

Table S21. Offset face-to-face $\pi\cdots\pi$ interactions in **1** at 100 K.

100 K	$\Theta^{[1]}$ (°)	$Z^{[2]}$ (Å)	100 K	Θ (°)	Z (Å)
L1-b ^[3] (C34 C35 N14 N15 O3) G1-a (C117 C118 C119 C120 C121 C122)	13.96	3.80	L4-a (C13 C14 C15 C16 C17 N5) G4-c (C83 C84 C93 C94 C95 C96)	5.44	3.82
L1-c (C36 C37 C38 C39 C40 N16) G1-d (C121 C122 C123 C124 C125 C126)	24.16	3.99	L4-a (C13 C14 C15 C16 C17 N5) G4-d (C84 C85 C90 C91 C92 C93)	7.58	3.99
L3-b (C6 C7 N2 N3 O1) G3-c (C69 C70 C71 C72 C73 C74)	12.05	3.72	L4-b (C18 C19 N6 N7 O2) G4-b (C81 C82 C83 C84 C85 C86)	2.11	3.64
L3-c (C8 C9 C10 C11 C12 N4) G3-b (C68 C69 C74 C75 C76 C77)	11.39	3.94	L3-b' (C6 C7 N2 N3 O1) G4-d (C84 C85 C90 C91 C92 C93)	7.02	3.49
L4-b (C18 C19 N6 N7 O2) G3-a (C67 C68 C77 C78 C79 C80)	6.84	3.59	L3-c' (C8 C9 C10 C11 C12) G4-a (C85 C86 C87 C88 C89 C90)	6.94	3.66
L4-a (C13 C14 C15 C16 C17 N5) G3-d (C65 C66 C67 C68 C69 C70)	12.17	3.98			

^[1] The dihedral angle between two aromatic rings; ^[2] The distance between the centroids of aromatic rings. ^[3] L and G denote the dpoda ligand and pyrene guest, respectively. Numbers and letters are used to mark different aromatic rings shown in Figure S20. Symmetry Codes: L3-b': $-1+x, y, z$.

Table S22. C-H···π interactions in **1** at 100 K.

100 K	$\Theta^{[1]} (\text{°})$	$Z^{[2]} (\text{\AA})$	100 K	$\Theta (\text{°})$	$Z (\text{\AA})$
G1-c ^[3] (C116 C117 C122 C123 C127 C128) G3-d (C65 C66 C67 C68 C69 C70)	80.78	4.85	G1-a (C117 C118 C119 C120 C121 C122) L4-a (C13 C14 C15 C16 C17 N5)	85.62	5.25
G2-b (C97 C98 C99 C100 C101 102) G4-a (C85 C86 C87 C88 C89 C90)	89.63	4.87	L4-a (C13 C14 C15 C16 C17 N5) L2-b' (C50 C51 N22 N23 O4)	75.49	5.41
G2-d (C100 C101 C106 C107 C108 C109) L3-c' (C8 C9 C10 C11 C12 N4)	83.45	5.14	L3-c' (C8 C9 C10 C11 C12 N4) L1-b' (C34 C35 N14 N15 O3)	69.77	5.31

^[1] The dihedral angle between two aromatic rings; ^[2] The distance between the centroids of aromatic rings. ^[3] L and G denote the dpoda ligand and pyrene guest, respectively. Numbers and letters are used to mark different aromatic rings shown in Figure S20. Symmetry Codes: L3-c': -1+x, y, z; L1-b': -1+x, 1/2+x, 1/2-y.

Table S23. Offset face-to-face $\pi\cdots\pi$ interactions in **2** at 100 K.

100 K	$\Theta^{[1]} (\text{°})$	$Z^{[2]} (\text{\AA})$	100 K	$\Theta (\text{°})$	$Z (\text{\AA})$
Part 1 ^[3]			Part 2		
L1-b ^[4] (C20 C21 N7 N8 O2) G1-a (C35 C36 C39 C40 C41 C42)	18.37	3.99	L1-b (C20 C21 N7 N8 O2) G1-a (C35 C36 C39 C40 C41 C42)	18.37	3.99
L3-b (C6 C7 N2 N3 O1) G3-c (C57 C58 C59 C60 C61 C62)	8.65	3.78	L3-b (C6 C7 N2 N3 O1) G3-c (C51A C52A C55A C56A C57A C58A)	4.72	3.79
L3-c (C1 C2 C3 C4 C5 N1) G3-b (C52 C53 C58 C59 C63 C64)	8.81	3.89	L3-c (C1 C2 C3 C4 C5 N1) G3-b (C49A C50A C51A C52A C53A C54A)	4.46	3.93
L3-b' (C6 C7 N2 N3 O1) G3-a (C49 C50 C51 C52 C53 C54)	8.24	3.56	L3-b' (C6 C7 N2 N3 O1) G3-a (C52A C53A C58A C59 C63A C64A)	3.30	3.67
L3-c' (C1 C2 C3 C4 C5 N1) G3-d (C51 C52 C55 C56 C57 C58)	6.88	3.89	L3-c' (C1 C2 C3 C4 C5 N1) G3-d (C57A C58A C59A C60A C61A C62A)	2.55	3.77

^[1] The dihedral angle between two aromatic rings; ^[2] The distance between the centroids of aromatic rings. ^[3] The pyrene guest G3 is disordered over two positions with a ratio of 50:50, which are shown in part 1 and part 2, respectively. ^[4] L and G denote the dpoda ligand and pyrene guest, respectively. Numbers and letters are used to mark different aromatic rings shown in Figure S21. Symmetry Codes: L3-b': -1/2+x, 1+y, 1/2-z.

Table S24. C-H···π interactions in **2** at 100 K.

100 K	$\Theta^{[1]} (\text{°})$	$Z^{[2]} (\text{\AA})$	100 K	$\Theta (\text{°})$	$Z (\text{\AA})$
Part 1 ^[3]			Part 2		
G1-c ^[4] (C36 C37 C42 C43 C47 C48) G3-d (C51 C52 C55 C56 C57 C58)	82.08	4.98	G1-c ^[4] (C36 C37 C42 C43 C47 C48) G3-d (C57A C58A C59A C60A C61A C62A)	86.66	4.97
L3-c' (C1 C2 C3 C4 C5 N1) L1-b'' (C20 C21 N7 N8 O2)	66.22	5.43	L3-c' (C1 C2 C3 C4 C5 N1) L1-b'' (C20 C21 N7 N8 O2)	66.07	5.23
G1-a (C35 C36 C39 C40 C41 C42) L3-c' (C1 C2 C3 C4 C5 N1)	89.11	5.32	G1-a (C35 C36 C39 C40 C41 C42) L3-c' (C1 C2 C3 C4 C5 N1)	89.11	5.32

^[1] The dihedral angle between two aromatic rings; ^[2] The distance between the centroids of aromatic rings. ^[3] The pyrene guest G3 is disordered over two positions with a ratio of 50:50, which are shown in part 1 and part 2, respectively. ^[4] L and G denote the dpoda ligand and pyrene guest, respectively. Numbers and letters are used to mark different aromatic rings shown in Figure S21. Symmetry Codes: L3-c': -1/2+x, 1+y, 1/2-z; L1-b'': 1/2-x, 1/2+y, z.

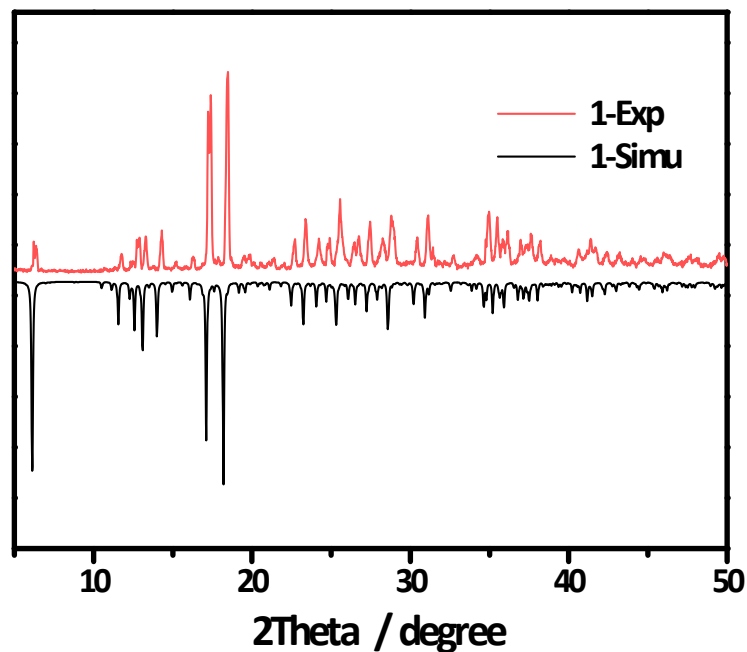


Figure S1. Powder X-ray diffraction (PXRD) pattern for **1** at 300 K and simulated PXRD pattern at 260 K. The peak shift may be due to different test temperatures.

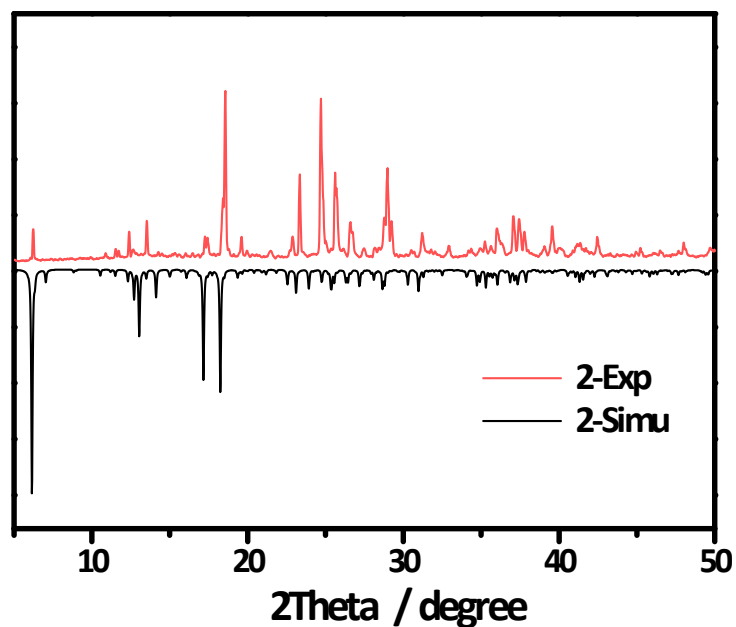


Figure S2. Powder X-ray diffraction (PXRD) pattern for **2** at 300 K and simulated PXRD pattern at 260 K. The peak shift may be due to different test temperatures.

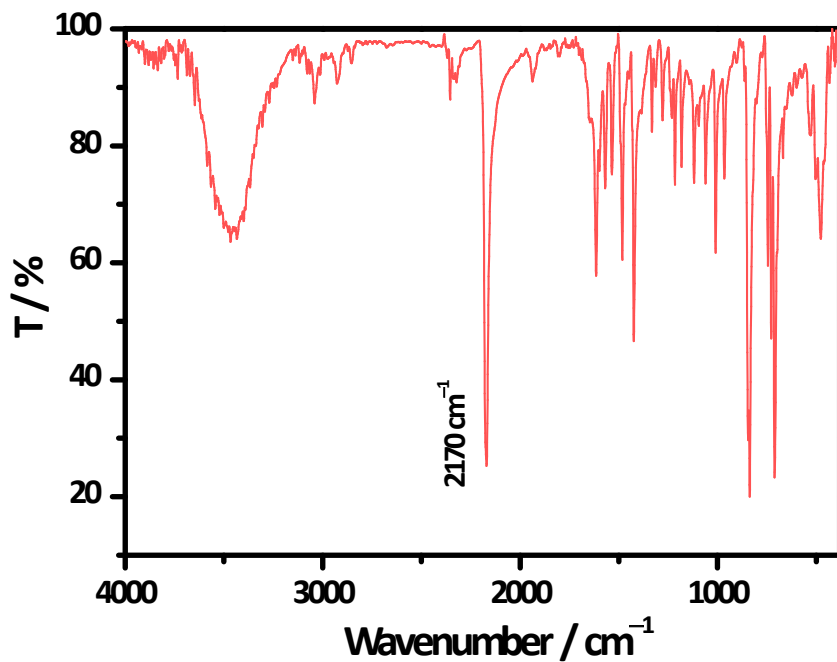


Figure S3. The FT-IR spectra of **1**. The characteristic band at 2170 cm⁻¹ in **1** is attributed to the stretching vibration of cyano group.

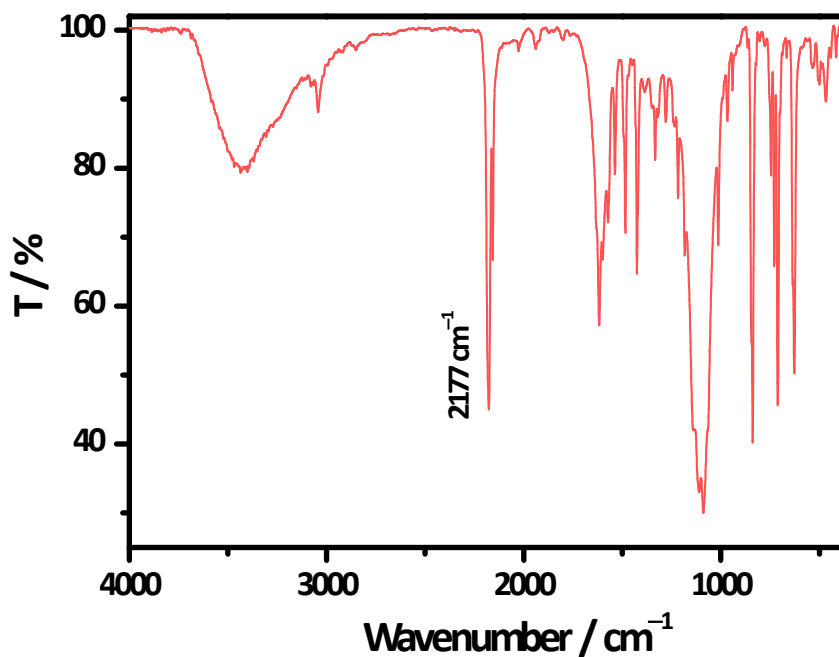


Figure S4. The FT-IR spectra of **2**. The characteristic band at 2177 cm⁻¹ in **2** is attributed to the stretching vibration of cyano group.

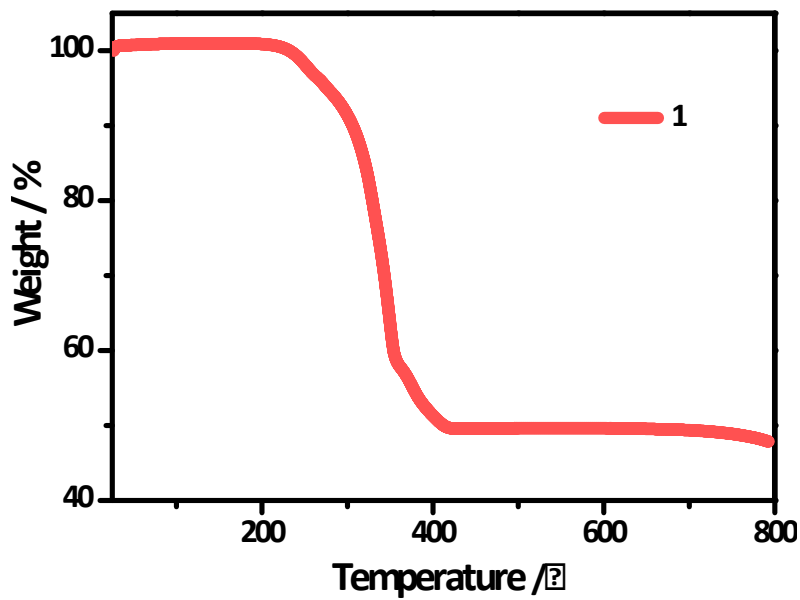


Figure S5. Thermogravimetric (TG) analysis curve of **1**.

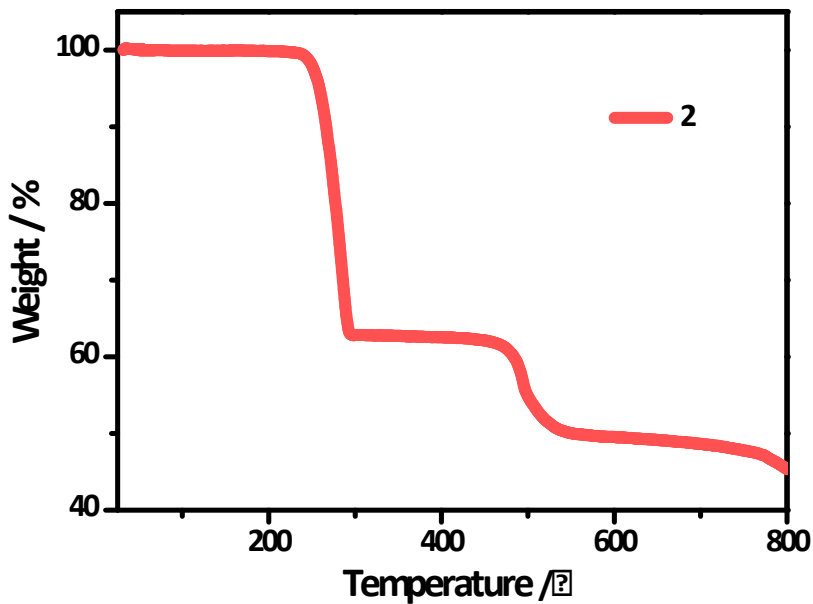


Figure S6. Thermogravimetric (TG) analysis curve of **2**.

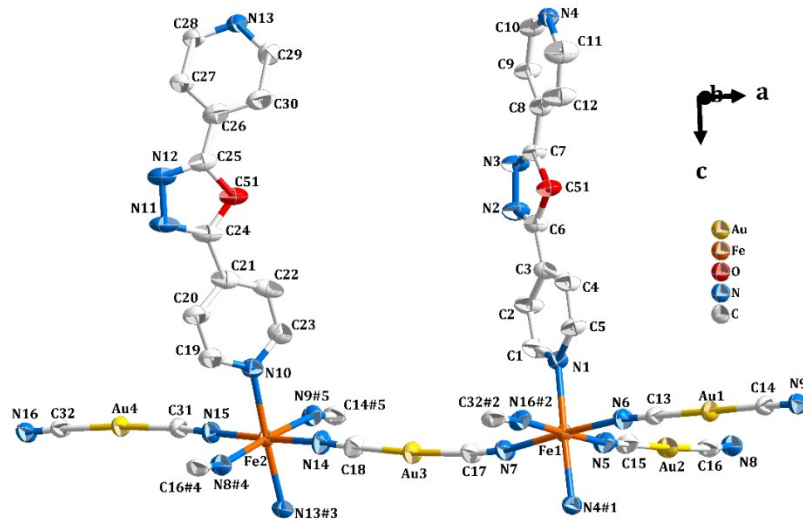


Figure S7. Asymmetric unit of **1** at 260 K. Thermal ellipsoids are drawn at the 50 % probability. Hydrogen atoms and pyrene guest molecules are omitted for clarity. Symmetric codes: #1: $x, 3/2-y, 1/2+z$; #2: $1/2-x, 1/2+y, z$; #3: $1/2-x, 1-y, 1/2+z$; #4: $-1+x, y, z$; #5: $3/2-x, -1/2+y, z$.

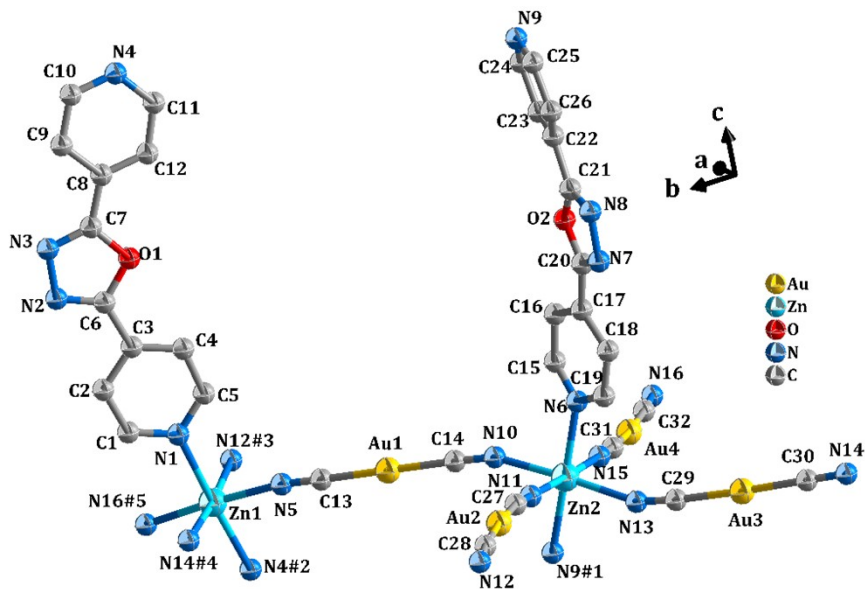


Figure S8. Asymmetric unit of **2** at 260 K. Thermal ellipsoids are drawn at the 50 % probability. Hydrogen atoms and pyrene guest molecules are omitted for clarity. The asymmetric units of **2** at 100, 145 and 198 K are similar to that at 260 K. Symmetric codes: #1: $1/2-x, 1-y, -1/2+z$; #2: $x, 3/2-y, -1/2+z$; #3: $1+x, y, z$; #4: $1/2-x, 1/2+y, z$; #5: $3/2-x, 1/2+y, z$.

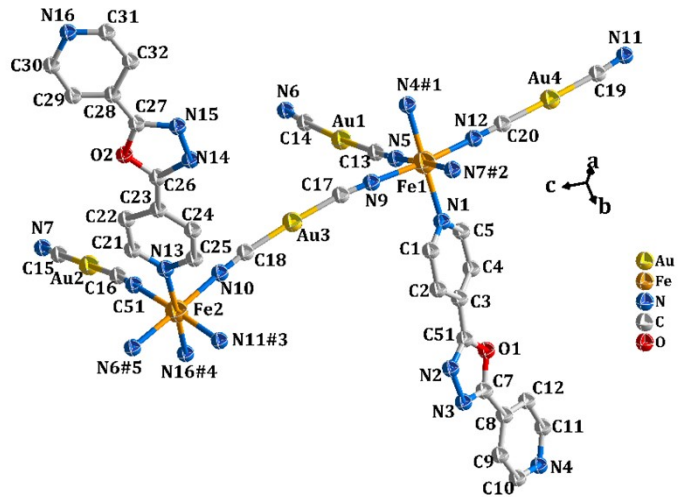


Figure S9. Asymmetric unit of **1** at 203 K. Thermal ellipsoids are drawn at the 50% probability. Hydrogen atoms and pyrene guest molecules are omitted for clarity. Symmetric codes: #1: $3/2-x, -1/2+y, z$; #2: $x, y, -1+z$; #3: $-1/2+x, y, 1/2-z$; #4: $1-x, 1/2+y, 3/2-z$; #5: $-1/2+x, y, 3/2-z$.

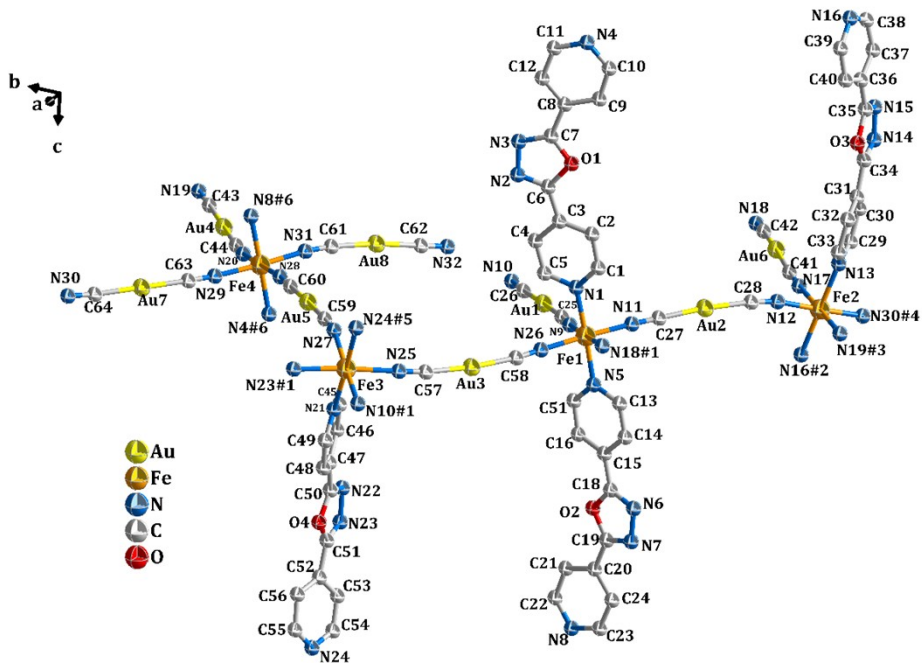


Figure S10. Asymmetric unit of **1** at 100 K. Thermal ellipsoids are drawn at the 50% probability. Hydrogen atoms and pyrene guest molecules are omitted for clarity. The asymmetric units of **1** at 145 and 198 K are similar to that at 100 K. Symmetric codes: #1: $1+x, y, z$; #2: $1/2-x, 1-y, 1/2+z$; #3: $x, -1+y, z$; #4: $-1+x, -1+y, z$; #5: $5/2-x, 2-y, -1/2+z$; #6: $3/2-x, 2-y, -1/2+z$.

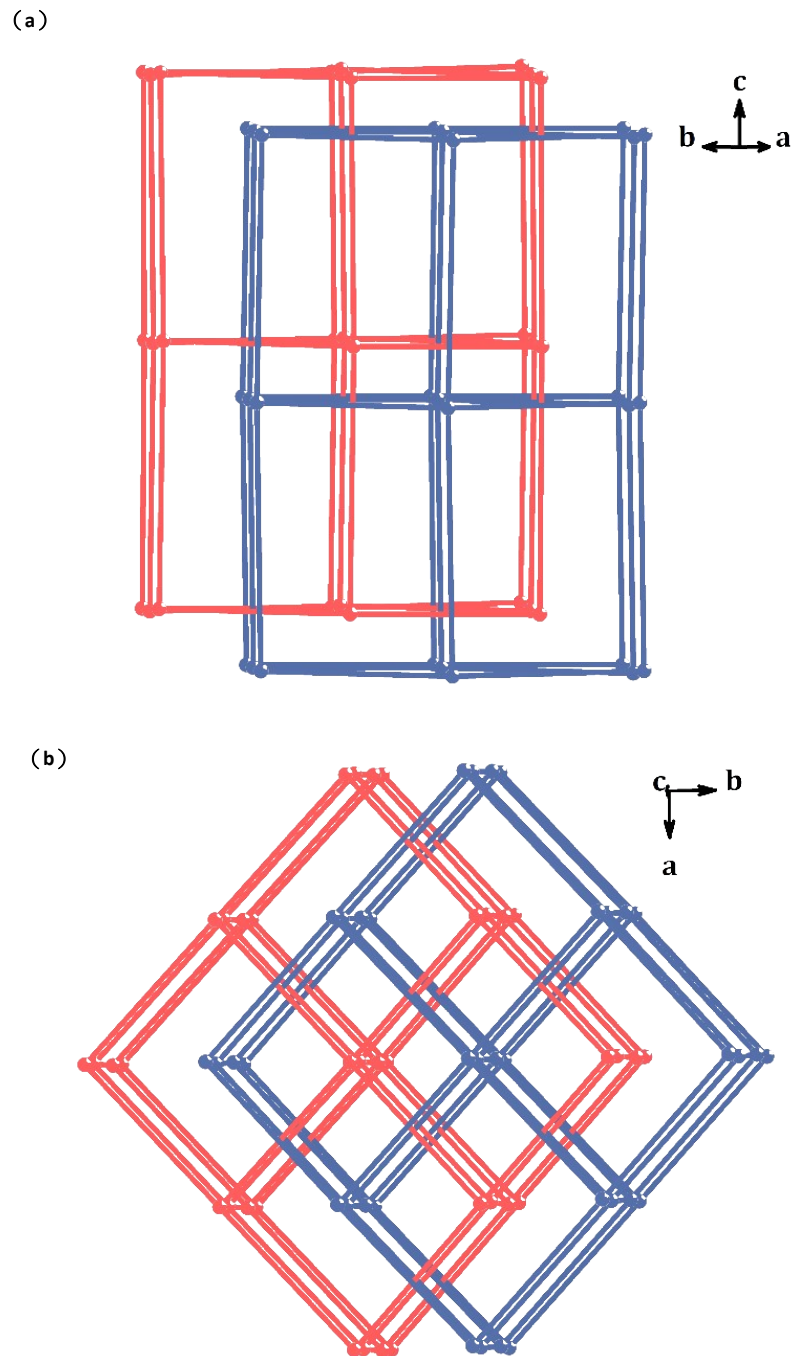


Figure S11. Views of two-fold interpenetrated frameworks with *pcu* type topology.

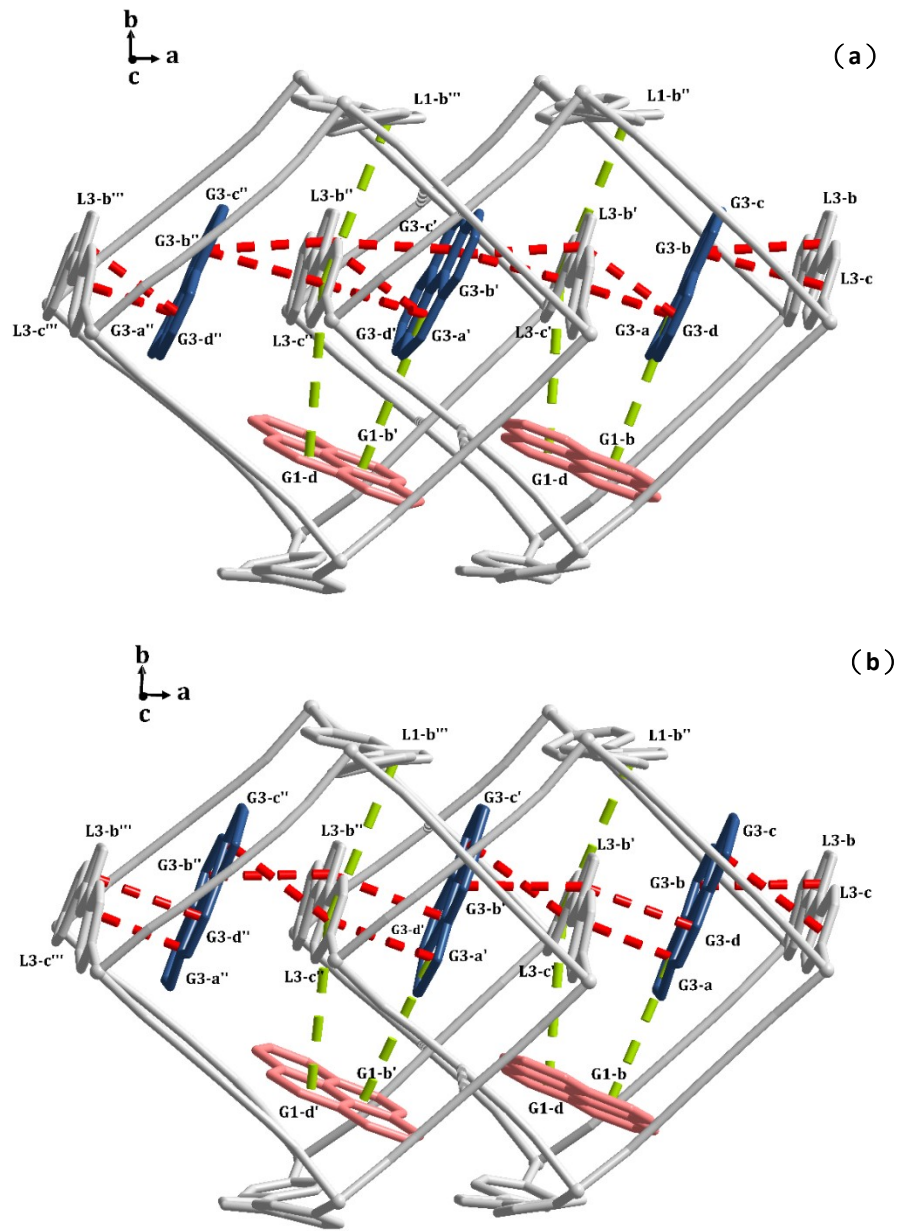


Figure S12. Structural representations of offset face-to-face $\pi\cdots\pi$ interactions (red dashed lines) and C-H $\cdots\pi$ interactions (green dashed lines) in **1** at 260 K. The pyrene guest G3 is disordered over two positions with a ratio of 39:61, which are shown in (a) and (b), respectively. Hydrogen atoms are omitted for clarity. The interpenetrated frameworks are shown in gray. Two crystallographically unique pyrene guests are distinguished by different colors.

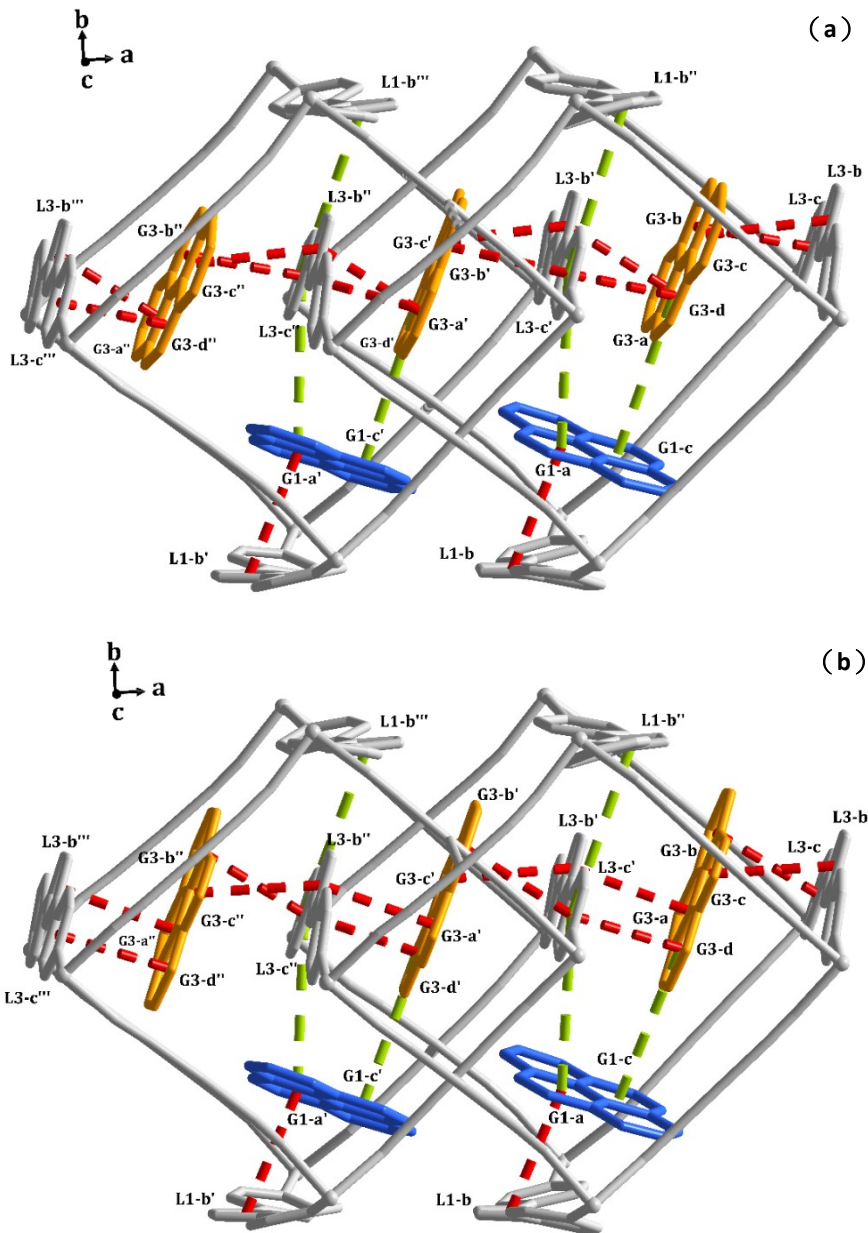


Figure S13. Structural representations of offset face-to-face $\pi\cdots\pi$ interactions (red dashed lines) and C-H $\cdots\pi$ interactions (green dashed lines) in **2** at 260 K. The pyrene guest G3 is disordered over two positions with a ratio of 50:50, which are shown in (a) and (b), respectively. Hydrogen atoms are omitted for clarity. The interpenetrated frameworks are shown in gray. Two crystallographically unique pyrene guests are distinguished by different colors.

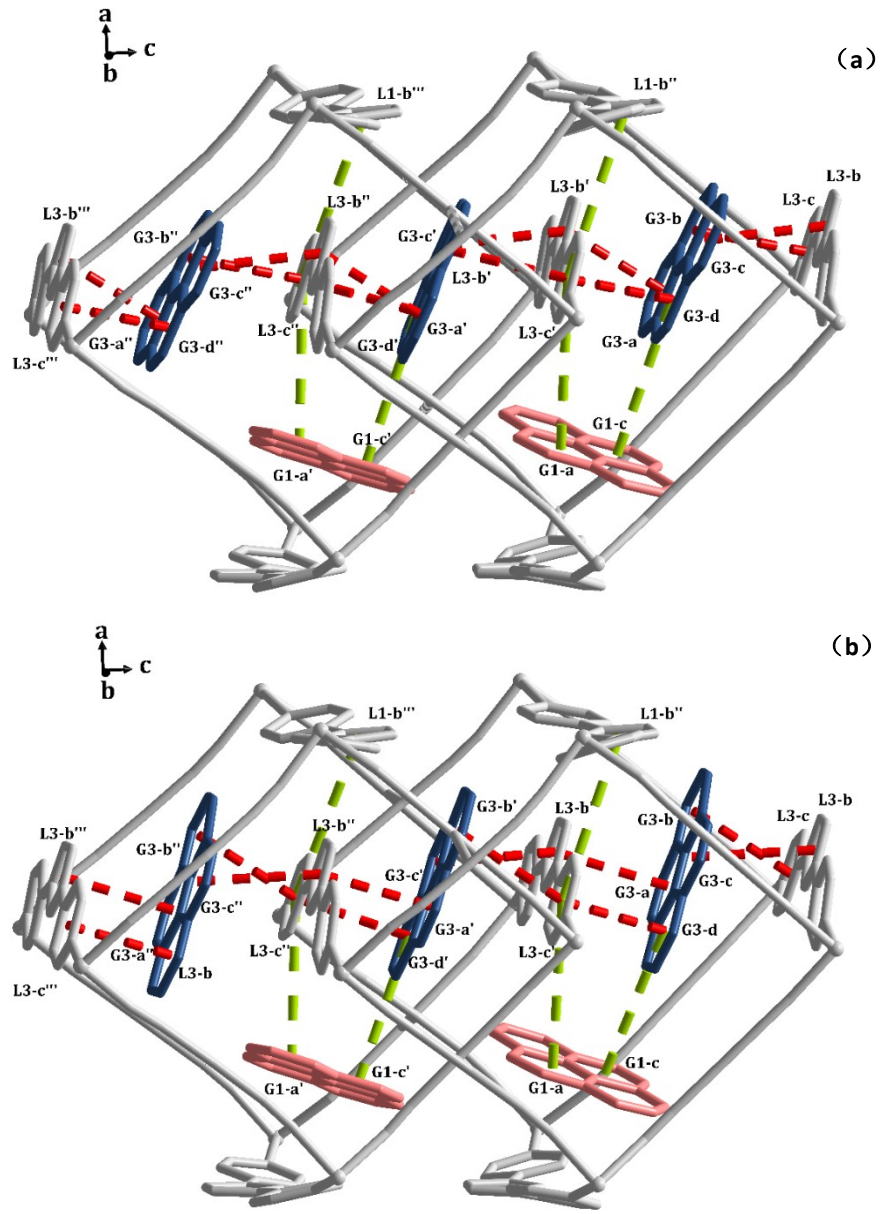


Figure S14. Structural representations of offset face-to-face $\pi\cdots\pi$ interactions (red dashed lines) and C-H $\cdots\pi$ interactions (green dashed lines) in **1** at 203 K. The pyrene guest G3 is disordered over two positions with a ratio of 59:41, which are shown in (a) and (b), respectively. Hydrogen atoms are omitted for clarity. The interpenetrated frameworks are shown in gray. Two crystallographically unique pyrene guests are distinguished by different colors.

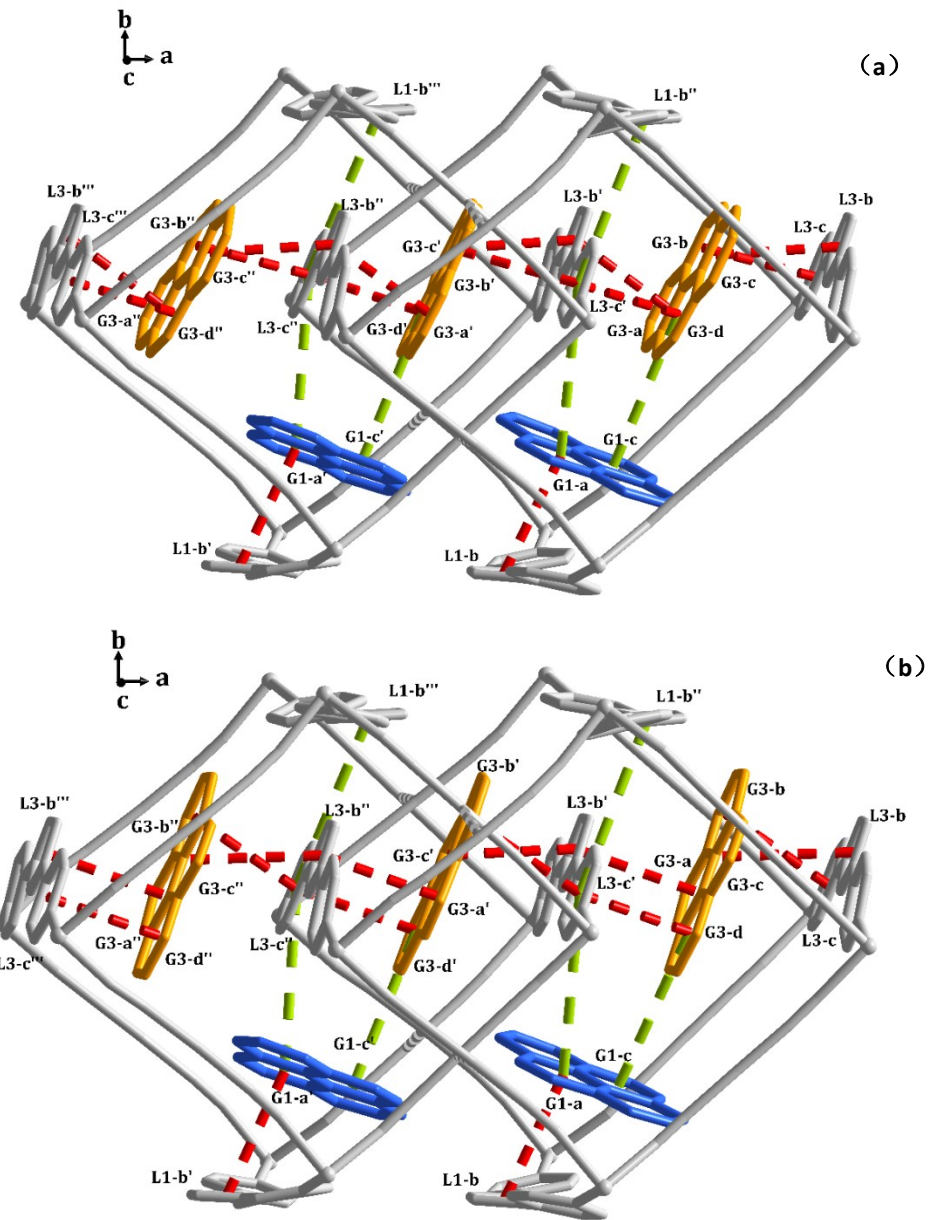


Figure S15. Structural representations of offset face-to-face $\pi\cdots\pi$ interactions (red dashed lines) and C-H $\cdots\pi$ interactions (green dashed lines) in **2** at 203 K. The pyrene guest G3 is disordered over two positions with a ratio of 50:50, which are shown in (a) and (b), respectively. Hydrogen atoms are omitted for clarity. The interpenetrated frameworks are shown in gray. Two crystallographically unique pyrene guests are distinguished by different colors.

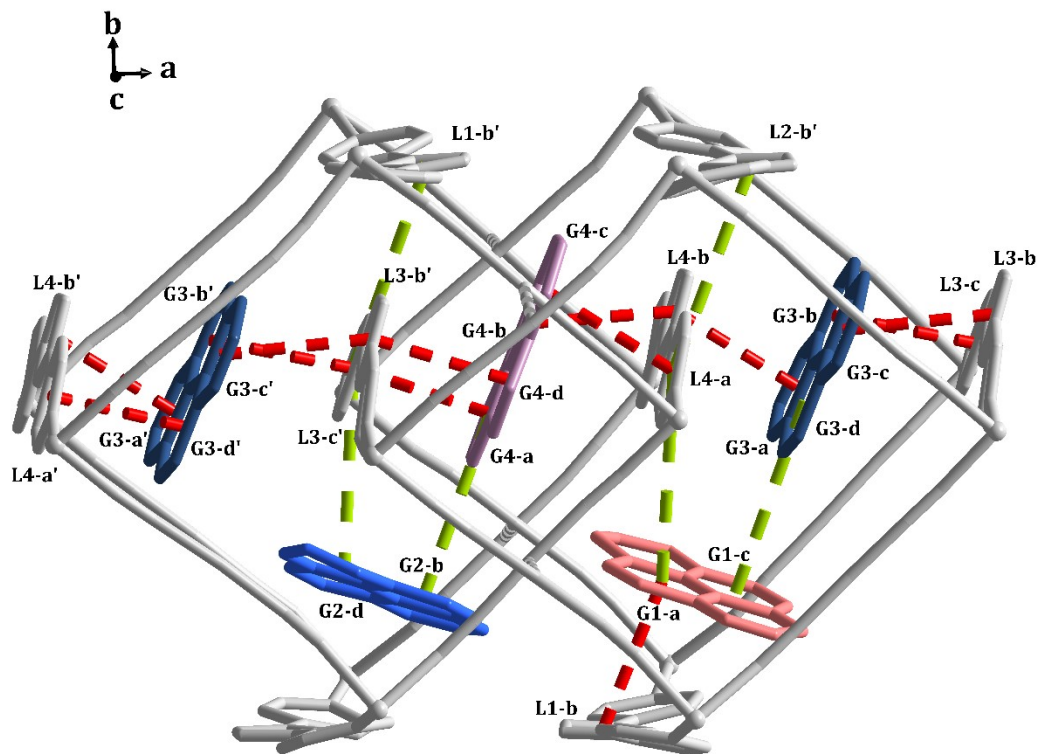


Figure S16. Structural representations of offset face-to-face $\pi\cdots\pi$ interactions (red dashed lines) and C-H $\cdots\pi$ interactions (green dashed lines) in **1** at 198 K. Hydrogen atoms are omitted for clarity. The interpenetrated frameworks are shown in gray. Four crystallographically unique pyrene guests are distinguished by four different colors.

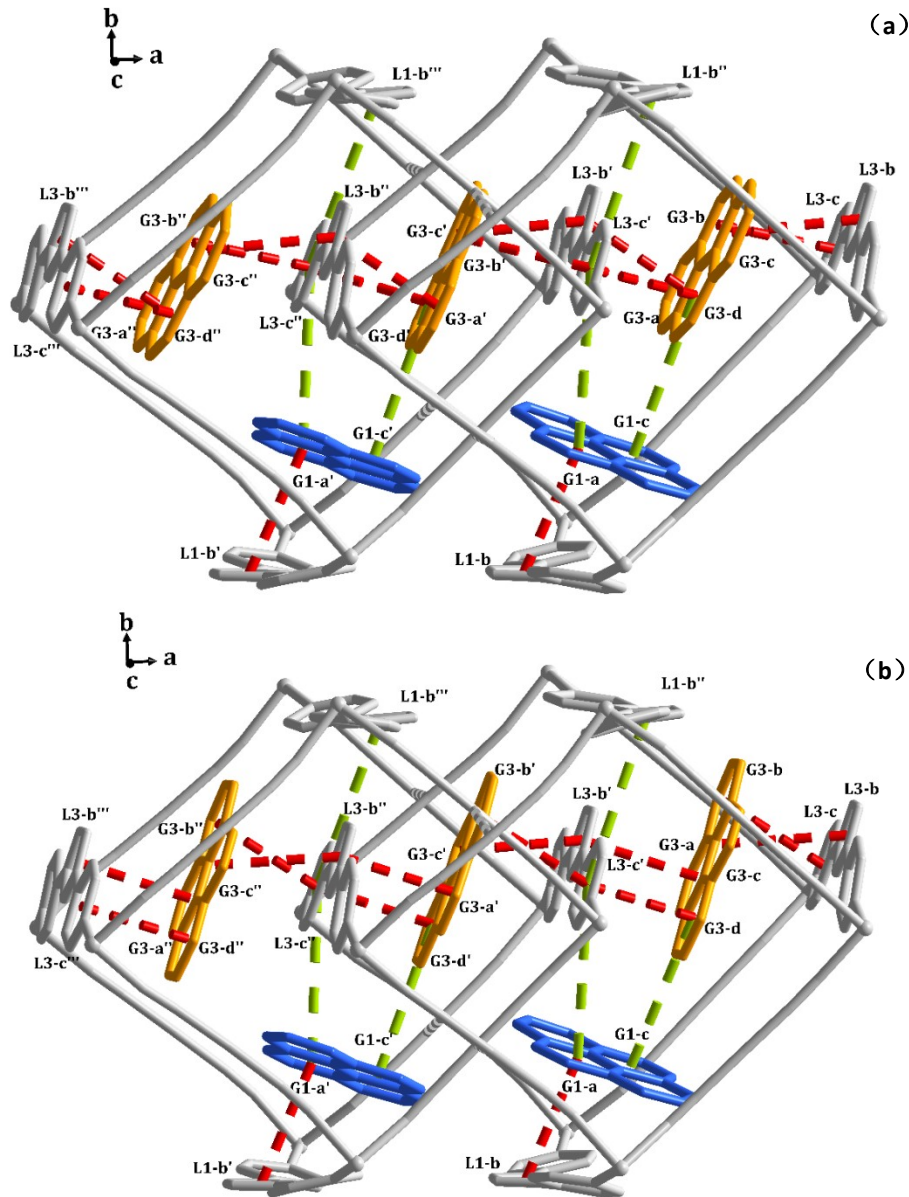


Figure S17. Structural representations of offset face-to-face $\pi\cdots\pi$ interactions (red dashed lines) and C-H $\cdots\pi$ interactions (green dashed lines) in **2** at 198 K. The pyrene guest G3 is disordered over two positions with a ratio of 50:50, which are shown in (a) and (b), respectively. Hydrogen atoms are omitted for clarity. The interpenetrated frameworks are shown in gray. Two crystallographically unique pyrene guests are distinguished by different colors.

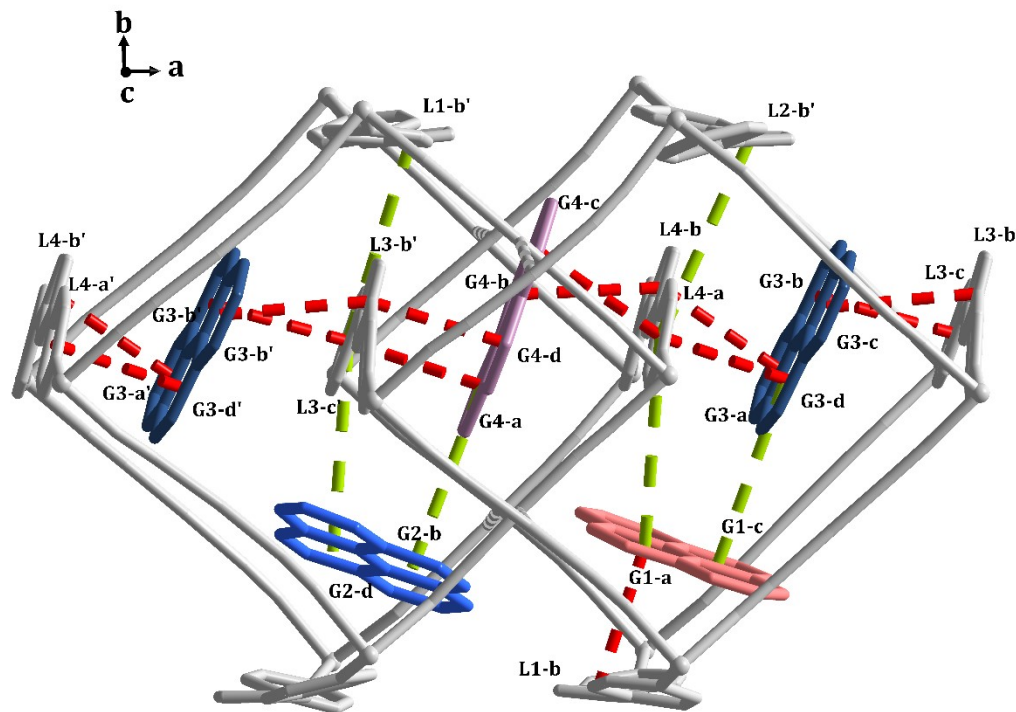


Figure S18. Structural representations of offset face-to-face $\pi\cdots\pi$ interactions (red dashed lines) and C-H $\cdots\pi$ interactions (green dashed lines) in **1** at 145 K. Hydrogen atoms are omitted for clarity. The interpenetrated frameworks are shown in gray. Four crystallographically unique pyrene guests are distinguished by four different colors.

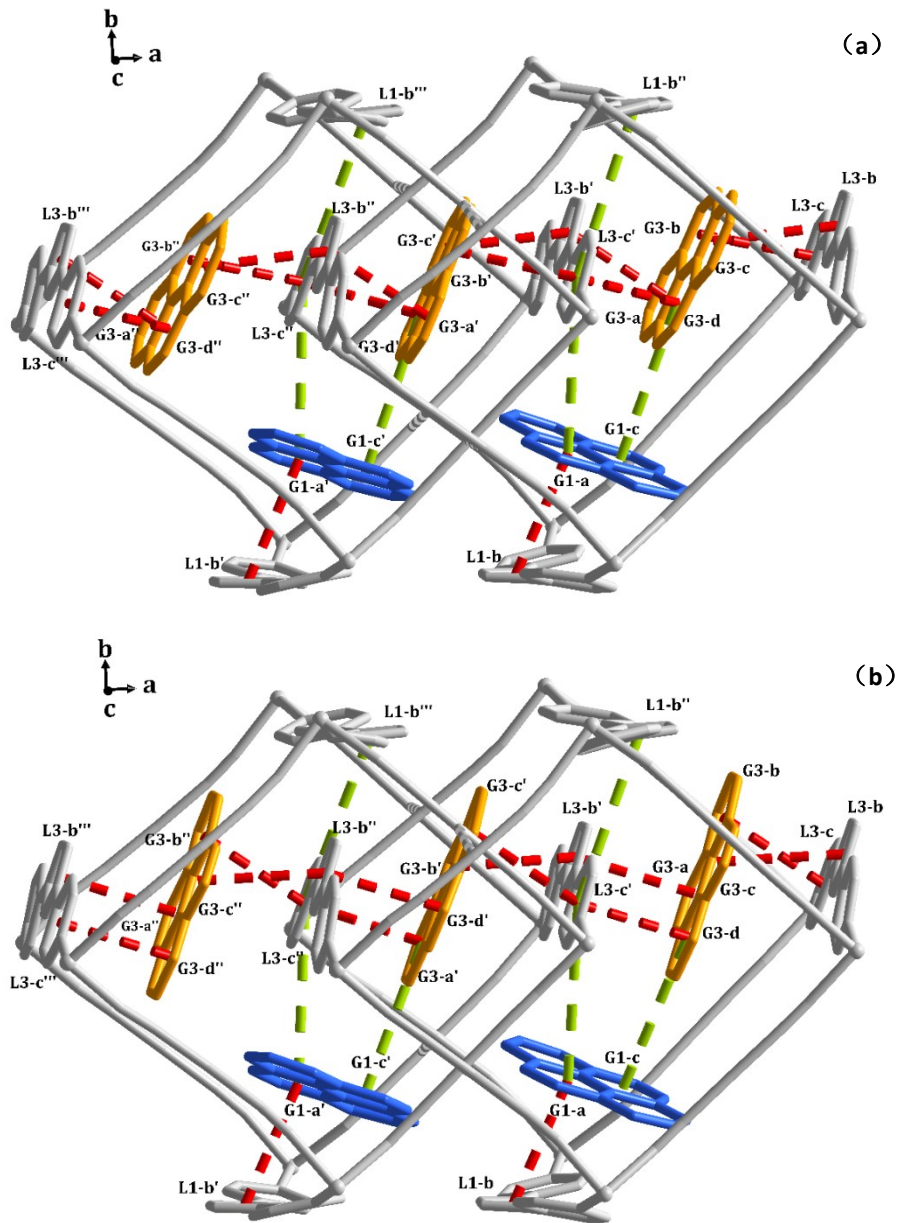


Figure S19. Structural representations of offset face-to-face $\pi\cdots\pi$ interactions (red dashed lines) and C-H $\cdots\pi$ interactions (green dashed lines) in **2** at 145 K. The pyrene guest G3 is disordered over two positions with a ratio of 50:50, which are shown in (a) and (b), respectively. Hydrogen atoms are omitted for clarity. The interpenetrated frameworks are shown in gray. Two crystallographically unique pyrene guests are distinguished by different colors.

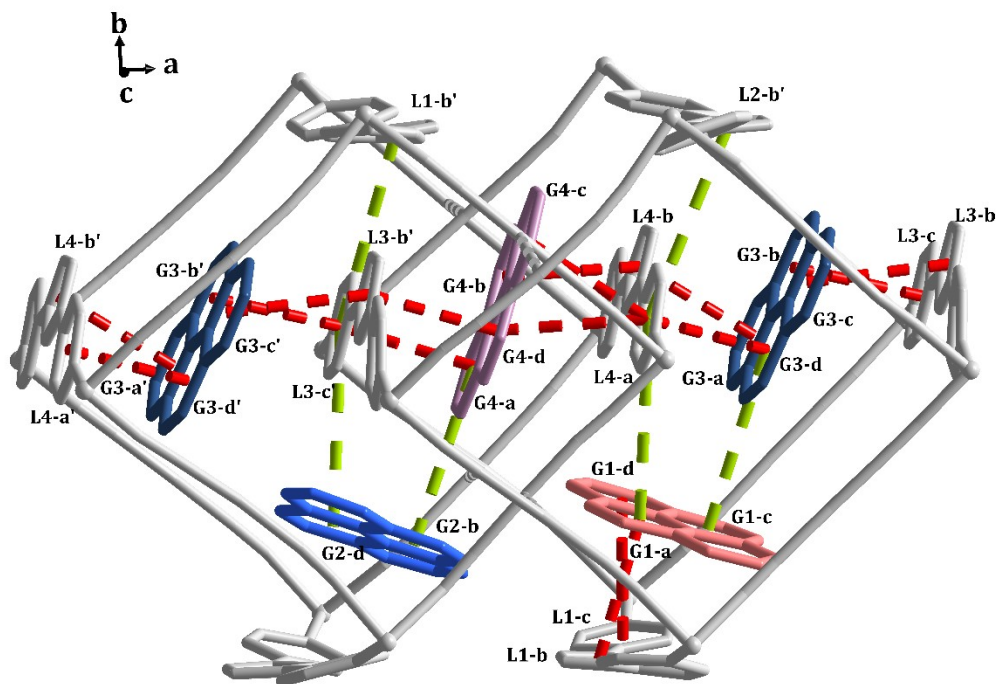


Figure S20. Structural representations of offset face-to-face $\pi\cdots\pi$ interactions (red dashed lines) and C-H $\cdots\pi$ interactions (green dashed lines) in **1** at 100 K. Hydrogen atoms are omitted for clarity. The interpenetrated frameworks are shown in gray. Four crystallographically unique pyrene guests are distinguished by four different colors.

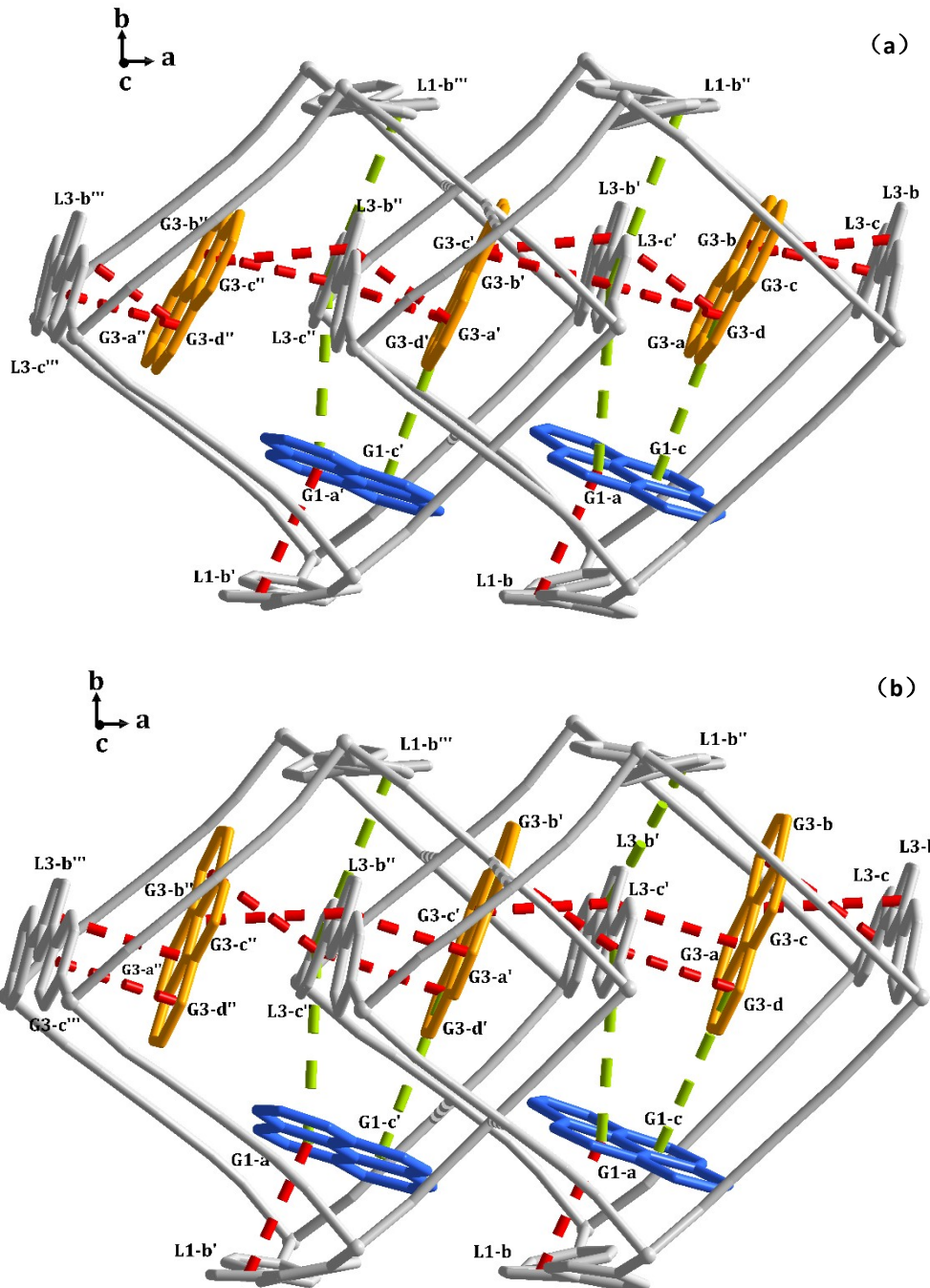


Figure S21. Structural representations of offset face-to-face $\pi\cdots\pi$ interactions (red dashed lines) and C-H $\cdots\pi$ interactions (green dashed lines) in **2** at 100 K. The pyrene guest G3 is disordered over two positions with a ratio of 50:50, which are shown in (a) and (b), respectively. Hydrogen atoms are omitted for clarity. The interpenetrated frameworks are shown in gray. Two crystallographically unique pyrene guests are distinguished by different colors.

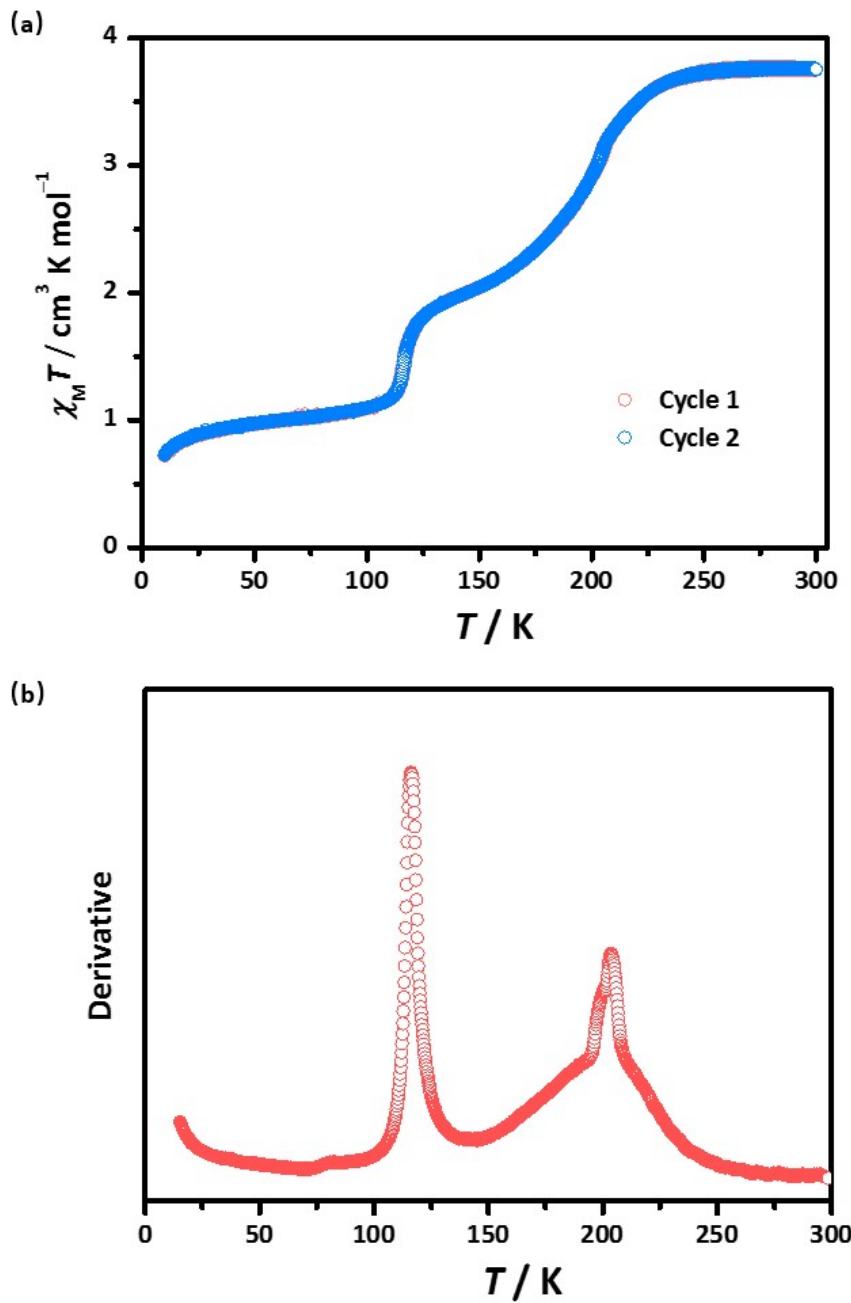


Figure S22. Two consecutive cycles of variable-temperature magnetic susceptibility data for **1** (a). The sweep rates are 5 and 2 K min⁻¹ for cycle 1 (red) and 2 (blue), respectively. The first derivative of magnetic susceptibility data (b).

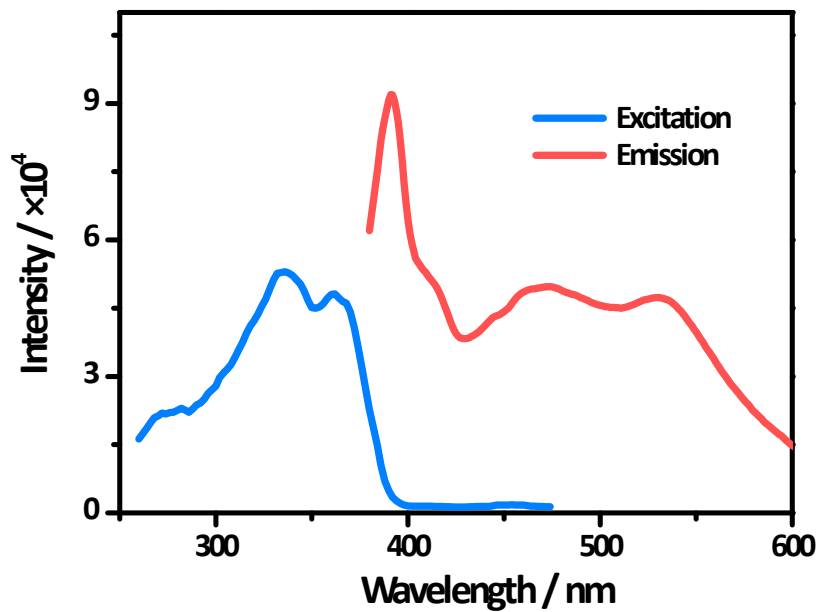


Figure S23. Solid-state fluorescence emission spectrum upon excitation at 338 nm and excitation spectrum monitored at 530 nm for **1** at room temperature.

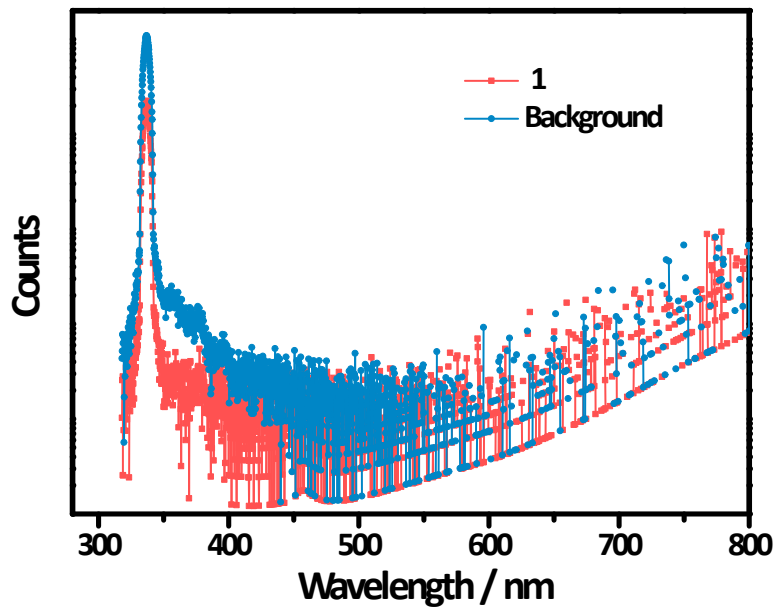


Figure S24. The fluorescence quantum yield of **1** in the solid state at room temperature. The low Φ_F value may be due to the quenching of Fe (II) ion.

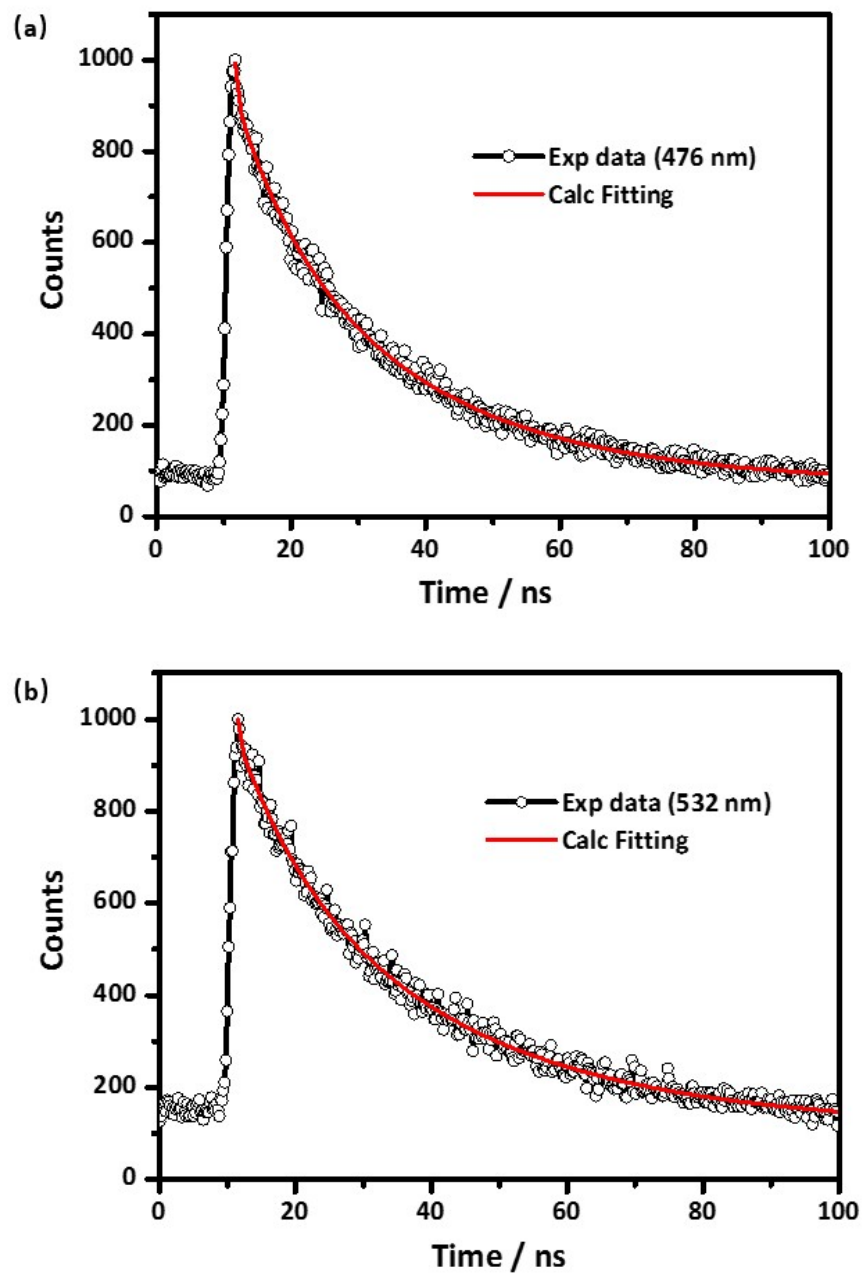


Figure S25. Fluorescence decay spectra of **1** in the solid state with an excitation wavelength of 338 nm monitored at 476 nm (a, $\tau = 21.18$ ns) and 532 nm (b, $\tau = 24.35$ ns) at room temperature.

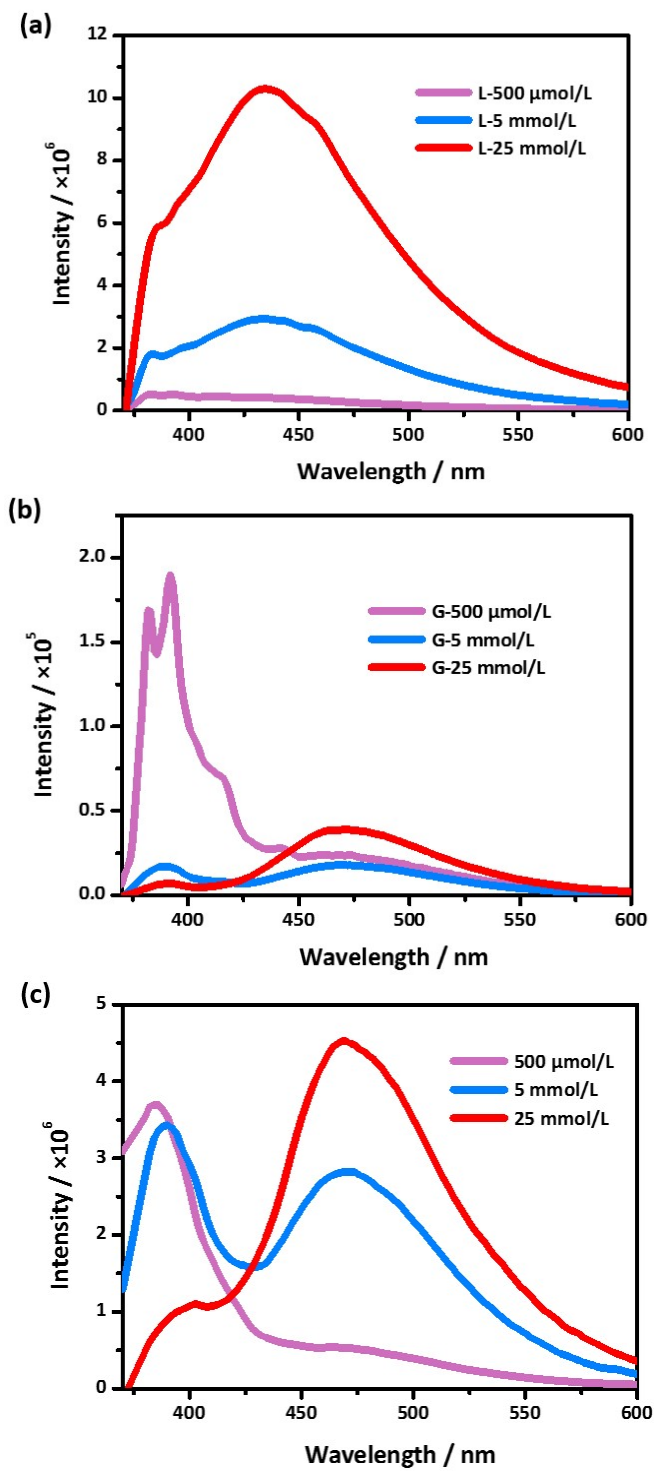


Figure S26. Fluorescence emission spectra of dpoda ligand (L) (a), pyrene guest (G) (b), and ligand-guest mixture with a ratio of 2:1 (c) at different concentrations (500 μ M, 5 mM, and 25 mM) in ethanol.

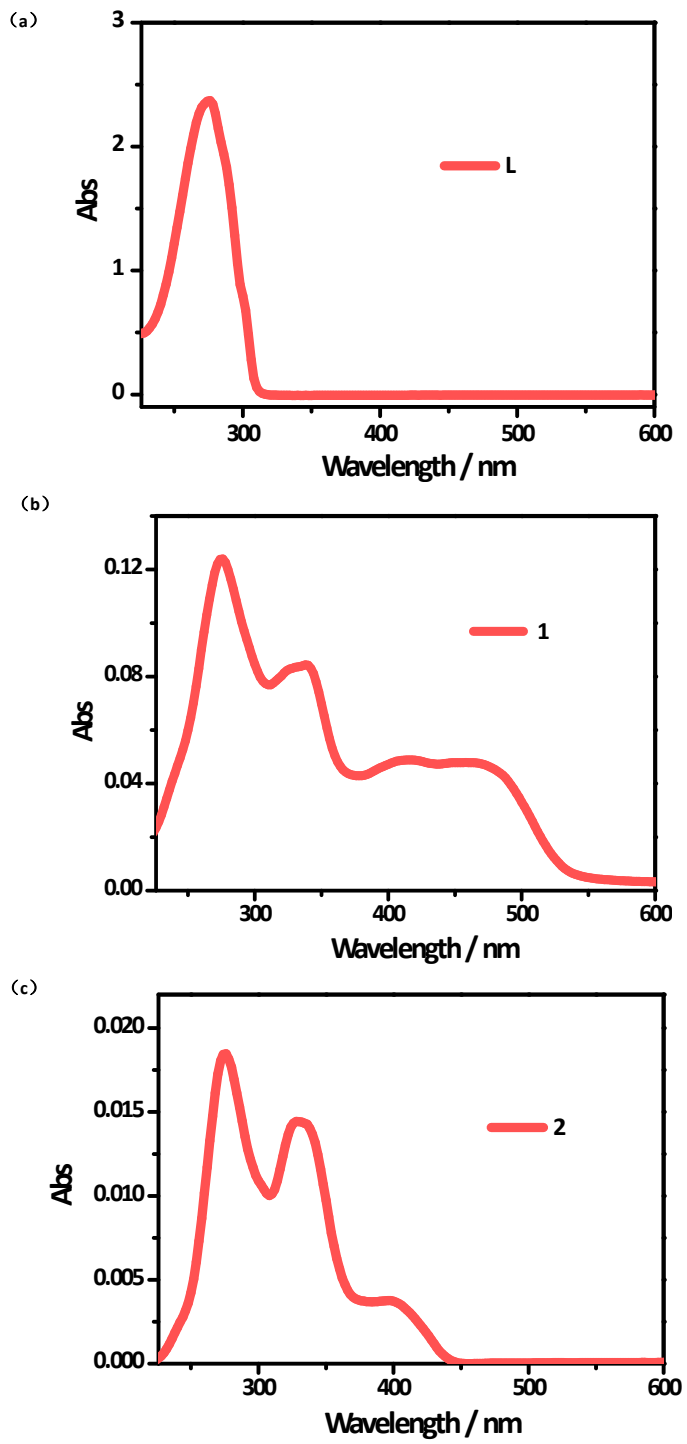


Figure S27 UV-visible absorption spectra of dpoda ligand in ethanol (a), **1** (b) and **2** (c) in the solid state at room temperature.

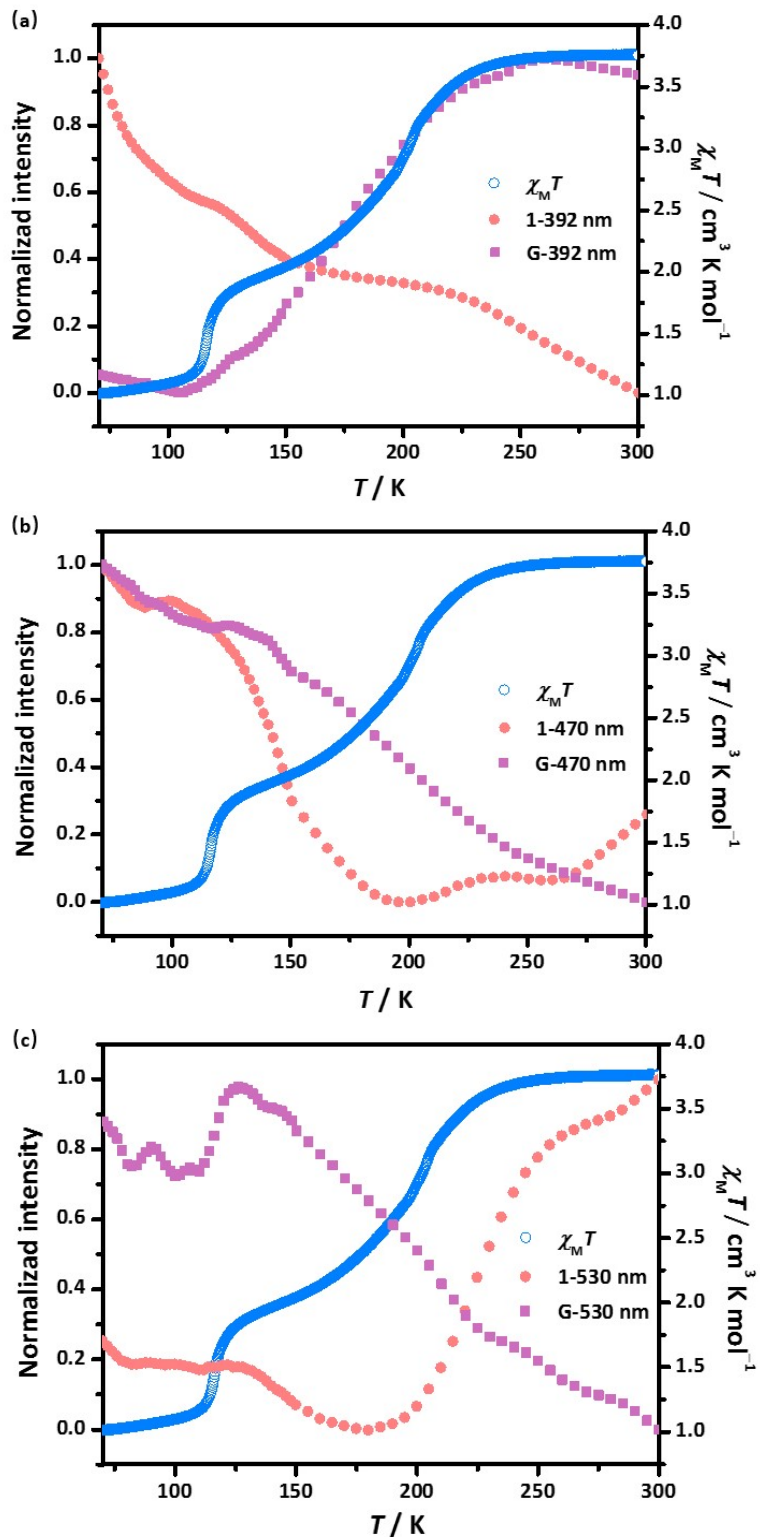


Figure S28. Temperature-dependent normalized fluorescence emission intensities at 392 nm (a), 470 nm (b) and 530nm (c) for **1** (orange) and pyrene guest (G, purple) compared with the magnetic data (blue).

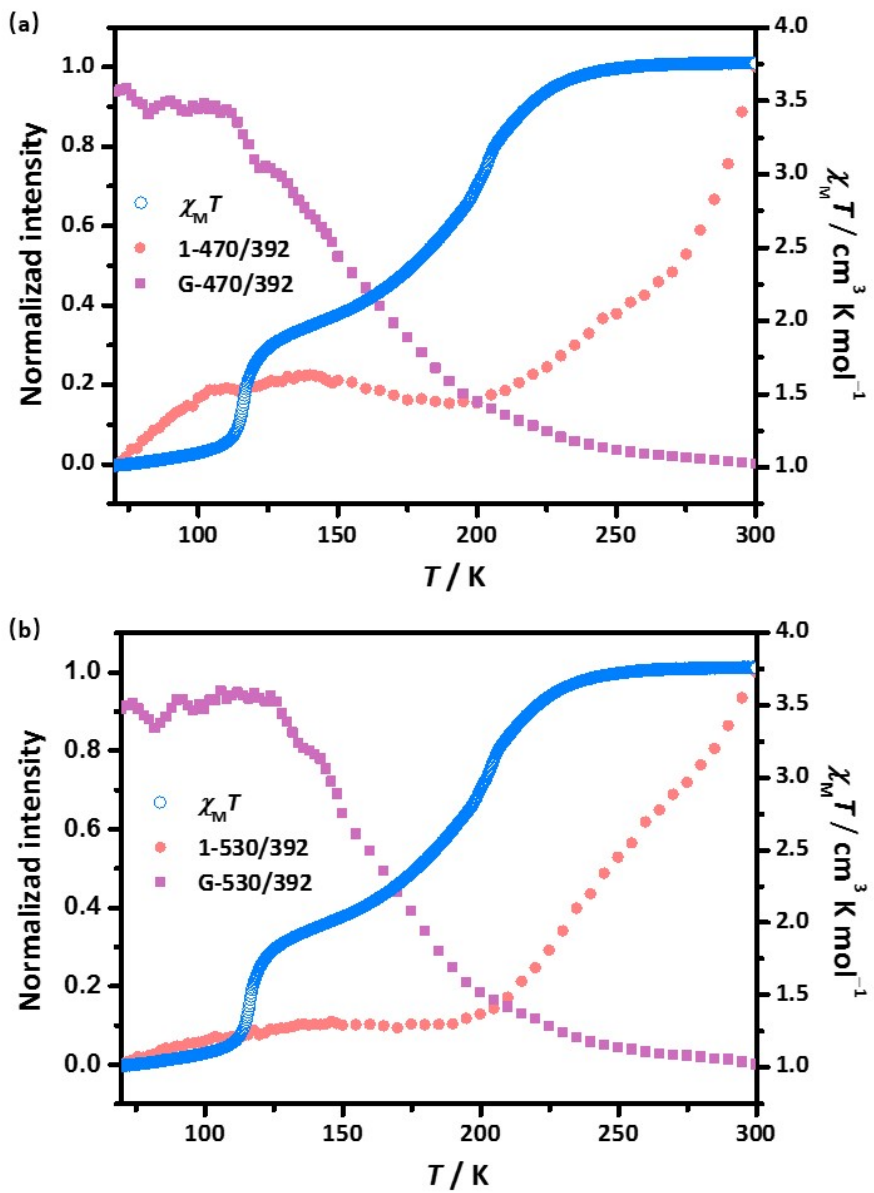


Figure S29. Temperature-dependent normalized fluorescence emission intensity ratios of 470 nm versus 392 nm (a) and 530 nm versus 392 nm (b) for **1** (orange) and pyrene guest (G, purple) compared with the magnetic data (blue).

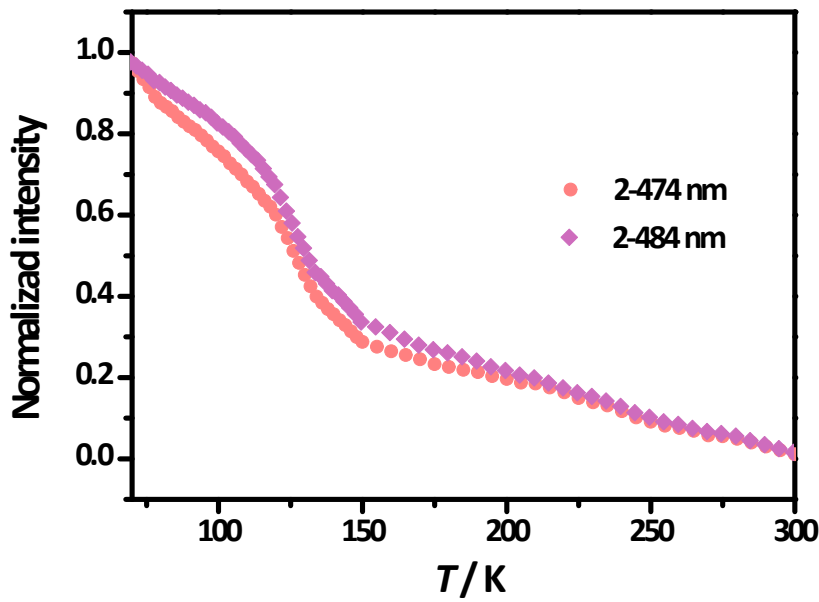


Figure S30. Temperature-dependent normalized fluorescence emission intensities at 474 and 484 nm for 2.

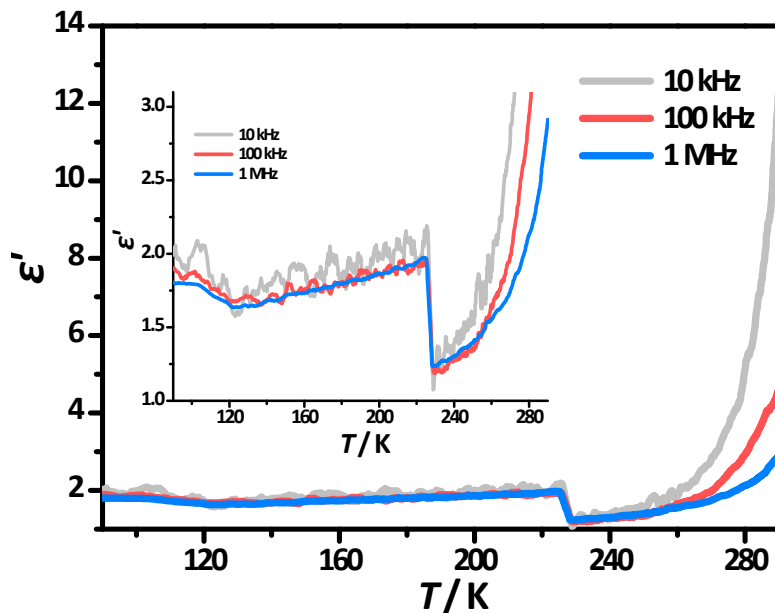


Figure S31. Variation of the dielectric constant of **1** at different frequencies (10 kHz, 100 kHz and 1 MHz) in the heating mode.

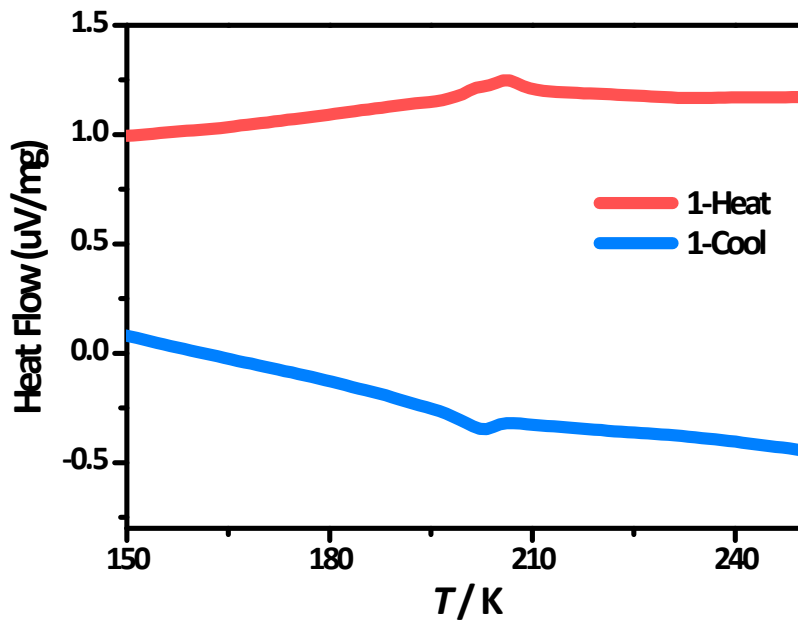


Figure S32. The differential scanning calorimetry (DSC) curves at 10 K min^{-1} for **1** in the cooling (blue) and heating (red) modes.